

## **Convective and wave signatures in ozone profiles over the equatorial Americas: Views from TC4 (2007) and SHADOZ**

Anne M. Thompson<sup>1</sup>, Alaina M. MacFarlane<sup>1,2</sup>, Gary A. Morris<sup>3</sup>, John E. Yorks<sup>1,4</sup>, Sonya K. Miller<sup>1</sup>, Brett F. Taubman<sup>5</sup>, Gé Verver<sup>6</sup>, Holger Vömel<sup>7</sup>, Melody A. Avery<sup>8</sup>, Johnathan W. Hair<sup>8</sup>, Glenn S. Diskin<sup>8</sup>, Edward V. Browell<sup>8</sup>, Jéssica Valverde Canossa<sup>8</sup>, Tom L. Kucsera<sup>10</sup>, Christopher A. Klich<sup>1</sup>, Dennis L. Hlavka<sup>4</sup>

<sup>1</sup> The Pennsylvania State University, Department of Meteorology

<sup>2</sup> Now at National Weather Service Middle Atlantic River Forecast Center

<sup>3</sup> Valparaiso University, Dept of Physics and Astronomy

<sup>4</sup> SSAI; also at NASA/Goddard Space Flight Center

<sup>5</sup> Appalachian State University, Dept of Chemistry

<sup>6</sup> KNMI (Royal Dutch Meteorological Institute)

<sup>7</sup> DWD- Deutscher Wetterdienst, GRUAN – Lindenberg

<sup>8</sup> NASA/Langley Research Center

<sup>9</sup> Laboratorio de Análisis Ambiental, Escuela de Ciencias Ambientales, Universidad Nacional

<sup>10</sup> Univ Maryland Baltimore County - GEST; also at NASA/Goddard

### **Popular Summary**

During the months of July-August 2007 NASA conducted a research campaign called the Tropical Composition, Clouds and Climate Coupling (TC4) experiment. Vertical profiles of ozone were measured daily using an instrument known as an ozonesonde, which is attached to a weather balloon and launch to altitudes in excess of 30 km. These ozone profiles were measured over coastal Las Tablas, Panamá (7.8N, 80W) and several times per week at Alajuela, Costa Rica (10N, 84W). Meteorological systems in the form of waves, detected most prominently in 100-300 m thick ozone layer in the tropical tropopause layer, occurred in 50% (Las Tablas) and 40% (Alajuela) of the soundings. These layers, associated with vertical displacements and classified as gravity waves (“GW,” possibly Kelvin waves), occur with similar structure and frequency over the Paramaribo (5.8N, 55W) and San Cristóbal (0.92S, 90W) sites of the Southern Hemisphere Additional Ozonesondes (SHADOZ) network. The gravity wave labeled layers in individual soundings correspond to cloud outflow as indicated by the tracers measured from the NASA DC-8 and other aircraft data, confirming convective initiation of equatorial waves. Layers representing quasi-horizontal displacements, referred to as Rossby waves, are robust features in soundings from 23 July to 5 August. The features associated with Rossby waves correspond to extra-tropical influence, possibly stratospheric, and sometimes to pollution transport. Comparison of Las Tablas and Alajuela ozone budgets with 1999-2007 Paramaribo and San Cristóbal soundings shows that TC4 is typical of climatology for the equatorial Americas. Overall during TC4, convection and associated meteorological waves appear to dominate ozone transport in the tropical tropopause layer.

Submitted to the TC4 Issue of JGR-Atmospheres (2009JD012909RR)

2 **Convective and wave signatures in ozone profiles over the equatorial**  
3 **Americas: Views from TC4 (2007) and SHADOZ**  
4

5 Anne M. Thompson,<sup>1</sup> Alaina M. MacFarlane,<sup>1,2</sup> Gary A. Morris,<sup>3</sup> John E. Yorks,<sup>1,4</sup> Sonya  
6 K. Miller,<sup>1</sup> Brett F. Taubman,<sup>5</sup> Gé Verver,<sup>6</sup> Holger Vömel,<sup>7</sup> Melody A. Avery,<sup>8</sup>  
7 Johnathan W. Hair,<sup>8</sup> Glenn S. Diskin,<sup>8</sup> Edward V. Browell,<sup>8</sup> Jéssica Valverde  
8 Canossa,<sup>9</sup> Tom L. Kucsera,<sup>10</sup> Christopher A. Klich,<sup>1</sup> Dennis L. Hlavka<sup>4</sup>  
9

10 <sup>1</sup> The Pennsylvania State University, Department of Meteorology, 503 Walker Building,  
11 University Park, PA 16802-5013 USA; [anne@met.psu.edu](mailto:anne@met.psu.edu); [smiller@psu.edu](mailto:smiller@psu.edu);  
12 [cok5018@psu.edu](mailto:cok5018@psu.edu)

13 <sup>2</sup> Now at National Weather Service Middle Atlantic River Forecast Center, State College, PA  
14 16803; [alaina.macfarlane@noaa.gov](mailto:alaina.macfarlane@noaa.gov)

15 <sup>3</sup> Valparaiso University, Dept of Physics and Astronomy, Valparaiso, IN 46383 USA;  
16 [gary.morris@valpo.edu](mailto:gary.morris@valpo.edu)

17 <sup>4</sup> SSAI of Lanham, MD 20706 USA; also at NASA/Goddard Space Flight Center, Greenbelt,  
18 MD 20771 USA; [john.e.yorks@nasa.gov](mailto:john.e.yorks@nasa.gov); [dennis.l.hlavka@nasa.gov](mailto:dennis.l.hlavka@nasa.gov)

19 <sup>5</sup> Appalachian State University, Dept of Chemistry, Boone, NC 28608; 828-262-7847;  
20 [taubmanbf@appstate.edu](mailto:taubmanbf@appstate.edu)

21 <sup>6</sup> KNMI (Royal Dutch Meteorological Institute), de Bilt, NL; [ge.verver@knmi.nl](mailto:ge.verver@knmi.nl)

22 <sup>7</sup> DWD- Deutscher Wetterdienst, GRUAN - Lindenberg, Germany; [Holger.voemel@dwd.de](mailto:Holger.voemel@dwd.de)

23 <sup>8</sup> NASA/Langley Research Center, MS 401B, Hampton, VA 23681;  
24 [melody.a.avery@nasa.gov](mailto:melody.a.avery@nasa.gov); [glenn.s.diskin@nasa.gov](mailto:glenn.s.diskin@nasa.gov); [johnathan.w.hair@nasa.gov](mailto:johnathan.w.hair@nasa.gov);  
25 [edward.v.browell@nasa.gov](mailto:edward.v.browell@nasa.gov)

26 <sup>9</sup> Laboratorio de Análisis Ambiental, Escuela de Ciencias Ambientales, Universidad Nacional  
27 P.O.Box: 86-3000 Heredia, Costa Rica; 00506-88694960; [jvalverde25@gmail.com](mailto:jvalverde25@gmail.com)

28 <sup>10</sup> Univ Maryland Baltimore County - GEST, Baltimore, MD 21228; also at NASA/Goddard  
29 Space Flight Center, 301-614-6046; [Tom.l.kucsera@nasa.gov](mailto:Tom.l.kucsera@nasa.gov)  
30

31 Keywords: Upper Troposphere/Lower Stratosphere; Ozonesondes; Tropical tropopause  
32 Layer; Gravity waves; Stratosphere-troposphere exchange

33 **Running Head - Thompson et. al.: TC4, SHADOZ O<sub>3</sub> & Waves**  
34 **Thompson et. al.: TC4, SHADOZ O<sub>3</sub> & Waves**

35 **Convective and wave signatures in ozone profiles over the equatorial**  
36 **Americas: Views from TC4 (2007) and SHADOZ**

37 **Abstract.** During the TC4 (Tropical Composition, Clouds and Climate Coupling)  
38 campaign in July-August 2007, daily ozonesondes were launched over coastal Las Tablas,  
39 Panamá (7.8N, 80W) and several times per week at Alajuela, Costa Rica (10N, 84W).  
40 Wave activity, detected most prominently in 100-300 m thick ozone laminae in the  
41 tropical tropopause layer, occurred in 50% (Las Tablas) and 40% (Alajuela) of the  
42 soundings. These layers, associated with vertical displacements and classified as gravity  
43 waves (“GW,” possibly Kelvin waves) by laminar identification, occur with similar  
44 structure and frequency over the Paramaribo (5.8N, 55W) and San Cristóbal (0.92S, 90W)  
45 Southern Hemisphere Additional Ozonesondes (SHADOZ) sites. GW-labeled laminae in  
46 individual soundings correspond to cloud outflow as indicated by DC-8 tracers and other  
47 aircraft data, confirming convective initiation of equatorial waves. Layers representing  
48 quasi-horizontal displacements, referred to as Rossby waves by the laminar technique, are  
49 robust features in soundings from 23 July to 5 August. The features associated with  
50 Rossby waves correspond to extra-tropical influence, possibly stratospheric, and  
51 sometimes to pollution transport. Comparison of Las Tablas and Alajuela ozone budgets  
52 with 1999-2007 Paramaribo and San Cristóbal soundings shows that TC4 is typical of  
53 climatology for the equatorial Americas. Overall during TC4, convection and associated  
54 waves appear to dominate ozone transport in the tropical tropopause layer; intrusions  
55 from the extra-tropics occur throughout the free troposphere.

56 **1. Introduction**

57 Ozone in the tropical troposphere reflects an interaction of photochemical and  
58 dynamical factors. The marine atmosphere is usually unpolluted, largely because the  
59 boundary layer (BL; see Appendix for abbreviations) is a region of O<sub>3</sub> photochemical loss  
60 [Piotrowicz *et al.*, 1991]. This is a consequence of slow formation (low NO<sub>x</sub> conditions;  
61 Zafiriou *et al.*, 1980; Thompson *et al.*, 1993) with loss by HO<sub>x</sub>, or occasionally by rapid O<sub>3</sub>  
62 destruction by halogens [Read *et al.*, 2008]. In the free troposphere mixed sources  
63 converge [Thompson *et al.*, 1996]. Advected pollution, stratospherically influenced air,  
64 and lightning add to O<sub>3</sub> formation, the latter at rates according to time since a lightning  
65 episode (Thompson *et al.*, 1997; see Cooper *et al.* [2006] and Bertram *et al.* [2007] for  
66 analyses of lightning influence in mid-latitudes). Extra-tropical ozone may also enrich  
67 ozone in the tropics [Randel *et al.*, 2007].

68 Examination of ozone profiles from sondes or aircraft over remote tropical sites  
69 reveals the free troposphere as a region of low O<sub>3</sub> (< 30 ppbv; Thompson *et al.*, 2003a)  
70 alternating with layers of elevated O<sub>3</sub> (sometimes > 100 ppbv; Newell *et al.*, 1999). From  
71 soundings taken through SHADOZ (Southern Hemisphere Additional Ozonesondes;  
72 Thompson *et al.*, 2003a,b; 2010; submitted article available as Supplemental Material),  
73 SOWER [Stratospheric Ozone and Water in Equatorial Regions; Hasebe *et al.*, 2007;  
74 Takashima and Shiotani, 2007] and related campaigns, much is known about the  
75 structure of O<sub>3</sub> in the tropical upper troposphere (UT) and lower stratosphere (LS). Stable  
76 pollution layers in the free troposphere are frequent over Réunion, Fiji, Samoa, San  
77 Cristóbal, and Ascension [Thompson *et al.*, 1996; 2003b; Oltmans *et al.*, 2001; 2004;  
78 Randriambelo *et al.*, 2003]. Reduced O<sub>3</sub> layers often characterize the UT and TTL  
79 (tropical tropopause layer, ~8-14 km; Fueglistaler *et al.*, 2009), where convective outflow  
80 of low-O<sub>3</sub> BL air occurs. If O<sub>3</sub> in the UT or TTL averages to lower concentrations than in  
81 the mid-troposphere, an “S-shape” profile results [Folkens *et al.*, 2000].

82 The laminar identification (LID) method, based on O<sub>3</sub> and potential temperature  
83 gradients [Teitelbaum *et al.*, 1994, 1996; Grant *et al.*, 1998; Thompson *et al.*, 2007a;  
84 2008], interprets persistent O<sub>3</sub> layers in terms of two wave-types. In the tropics, Rossby  
85 waves (RW) represent horizontal displacement; these correspond to filaments of extra-  
86 tropical air or pollution from long-range transport. When SHADOZ profiles are analyzed  
87 with the LID technique, RW signatures appear in < 20% of the soundings [Loucks, 2007;  
88 Thompson *et al.*, 2010]. Signatures of convectively-generated gravity waves (GW) occur

89 in 40-90% of SHADOZ soundings, depending on location and season [*Thompson et al.*,  
90 2010a,b]. Near the tropopause, GW are usually identified with Kelvin waves. Transient  
91 Kelvin waves have been observed in O<sub>3</sub> over both eastern and western Pacific [*Fujiwara et*  
92 *al.*, 1998; 2001].

93 Wave activity over the equatorial Americas has received less attention. Robust GW  
94 and RW signals were noted during the Milagro/INTEX-B/IONS-06 (Intercontinental  
95 Transport Experiment; INTEX Ozone-sonde Network Study) campaigns over Mexico City  
96 (19N, 99W) and Houston (30N, 95W) in March-May 2006 [*Thompson et al.*, 2008], two  
97 locations that are essentially sub-tropical when springtime air parcel flows link them to  
98 central America [*Fast et al.*, 2007]. The TC4 (Tropical Composition, Cloud, and Climate  
99 Coupling) mission in July-August 2007 offered an opportunity to characterize O<sub>3</sub> profiles  
100 closer to the equator than the IONS-06 soundings. TC4 [*Toon et al.*, 2010] investigated  
101 chemical transformation in convective systems and the impacts of deep convection on  
102 constituent transport, dehydration and cirrus formation. Sampling from San Jose, Costa  
103 Rica, with NASA's DC-8, WB-57 and ER-2 aircraft, was well-suited for comparisons with  
104 observations from Las Tablas, Panamá (LTP, 7.8N, 80W), where daily soundings were  
105 made from the NATIVE (Nittany Atmospheric Trailer and Integrated Validation  
106 Experiment) mobile lab. Most TC4 flights were south of the Intertropical Convergence  
107 Zone (ITCZ), which was located at 12-13N during the experiment [*Toon et al.*, 2010].  
108 SHADOZ [*Thompson et al.*, 2003a] soundings from Costa Rica (Alajuela, 10N,84W) were  
109 augmented with several launches per week from early July through 9 August 2007.

110 Five TC4 studies are devoted to analysis of ozone transport and wave activity. In  
111 *Selkirk et al.* [2010] temperature anomalies from four-times-daily radiosondes over  
112 Alajuela indicate equatorial waves in the TTL. Comparison of TC4 radiosondes and water  
113 vapor from cryogenic frost-point hygrometer readings suggests less convection than  
114 during the 2005 TCSP (Tropical Convective Systems and Processes) campaign in the  
115 same location and time of year. The free troposphere was drier in TC4 than TCSP, and O<sub>3</sub>  
116 in the mid-upper troposphere was ~35% higher in TC4 (Figures 1, 3 and 4 in *Selkirk et*  
117 *al.*, 2010). *Avery et al.* [2010] focus on the strong anti-correlation between ozone and  
118 condensed cloud water content measured during sampling in active convection, and  
119 generalize their findings on convective redistribution of ozone with tracer composites.  
120 Convective outflow as indicated by local O<sub>3</sub> minima and elevated lower tropospheric  
121 tracers appears to maximize at 10-11 km. *Avery et al.* [2010] argue that in the DC-8

122 sampling region near the ITCZ, there has been about 50% convective turnover below the  
123 TTL, with vertical transport from just above the boundary layer. In *Morris et al.* [2010]  
124 lower-mid tropospheric O<sub>3</sub> within a convectively active region over the Pacific southwest  
125 of the Las Tablas (LTP) launch site on 5 August 2007 is investigated in detail. The LTP  
126 sounding for that day was caught in a strongly convective cell that bounced the balloon  
127 package up and down between 2.5-5 km; the O<sub>3</sub> within this layer increased from 30 to 40  
128 ppbv before the balloon ascended to the stratosphere. *Petropavlovskikh et al.* [2010],  
129 analyzing the 17 July 2007 DC-8 flight, find that influences on O<sub>3</sub> near the TTL are a  
130 mixture of convection and advection, the latter including extra-tropical air, some of it  
131 possibly of stratospheric origins. The lowest O<sub>3</sub> layer occurred at 9-11 km, but low-O<sub>3</sub>  
132 signatures were also recorded by the UV-DIAL instrument at 2-4 km and 13 km.

133 As insightful as the above investigations are, none systematically examines  
134 dynamic influences in ozone structure in the free troposphere and LS day-by-day during  
135 TC4. That is the purpose of the present study. Using the full record of Alajuela (ACR)  
136 and Las Tablas O<sub>3</sub> soundings (**Section 2**), the following analyses are performed:

137 1) Mean O<sub>3</sub> profiles are determined and day-to-day variability is examined in  
138 curtains of O<sub>3</sub> mixing ratio and in integrated O<sub>3</sub> column amounts.

139 2) Ozone budgets based on LID and expressed as amounts affected by GW and  
140 RW provide a consistent framework for examining dynamic influences over the course of  
141 TC4. The climatology of wave signatures at LTP and ACR is compared to those at  
142 Paramaribo (5.8N,55W) and San Cristóbal (0.92S,90W) sondes, long-term SHADOZ  
143 stations also in the equatorial Americas (**Section 3.1**).

144 3) Case studies of soundings and ancillary aircraft measurements are used to  
145 corroborate wave designations, with convection for GW and stratospheric influences or  
146 pollution for RW (**Section 3.2**). One episode is among those analyzed by *Avery et al.*  
147 [2010] and *Morris et al.* [2010]. Others were chosen to illustrate contrasting impacts.

148 4) In **Section 4** context for the TC4 observations is given by June-July-August  
149 (JJA) Costa Rican sondes in 2006, and the 9-year SHADOZ record [*Thompson et al.*,  
150 2003a,b] at Paramaribo and San Cristóbal. Specifically we ask:

- 151 > How does tropospheric O<sub>3</sub> over LTP and ACR in 2007 compare to JJA O<sub>3</sub> over  
152 Costa Rica (Heredia site near Alajuela) in 2006, when an El Niño affected  
153 the eastern Pacific [*Arguez, 2007*]? How do LTP and ACR O<sub>3</sub> during TC4  
154 compare to O<sub>3</sub> over San Cristóbal in 2007?

155 > How does O<sub>3</sub> over the equatorial Americas in TC4 compare to the 1999-2006  
156 record? Indices based on GW activity are used to quantify interannual  
157 variability.

## 158 **2. Experimental. Observations and Methods of Analysis.**

### 159 2.1 Ground & Aircraft

160 Continuous surface O<sub>3</sub> measurements at Las Tablas (7.8N,80W) were made during  
161 the period 13 July to 10 August 2007 from the NATIVE mobile lab that also included an  
162 ozonesonde ground station. The surface O<sub>3</sub> was measured with a TECO Model 49 C ozone  
163 analyzer, along with carbon monoxide (TECO Model 48CTL), NO and NO<sub>y</sub> (TECO Model  
164 42CY), SO<sub>2</sub> (TECO Model 43C-TLE) and particle size distribution (Scanning Mobility  
165 Particle Sizer). All data can be viewed at <[http://ozone.met.psu.edu/NATIVE/  
166 measurements.html](http://ozone.met.psu.edu/NATIVE/measurements.html)>. Calibrations of O<sub>3</sub>, CO, and SO<sub>2</sub> were made prior to and directly  
167 after the campaign with instrument grade gases (Airgas, Inc.). Calibration of NO and NO<sub>y</sub>  
168 was performed daily with instrument grade NO (Airgas, Inc.). Catalytic conversion  
169 efficiency tested before and after TC4 remained close to 100%.

### 170 2.2 Ozone Profiles and P-T-U Profiles

171 All ozone profile data analyzed here were taken with electrochemical concentration  
172 cell (ECC) instruments coupled with standard radiosondes, as described in *Thompson et*  
173 *al.* [2003; 2007a]. Coordinates of LTP, ACR and the SHADOZ sites referred to here  
174 appear in **Table 1**, along with details of the sondes used. At Las Tablas, the 0.5% KI  
175 buffered solution with ENSCI ozonesondes is a combination that optimizes tropospheric  
176 and stratospheric O<sub>3</sub> measurements [Smit *et al.*, 2007; *Thompson et al.*, 2007b; *Deshler*  
177 *et al.*, 2008]. Vaisala radiosondes, Model RS-80, were used to collect P-T-U data. For  
178 nine of the 25 LTP soundings during TC4 the humidity data are unreliable above ~300-  
179 500 hPa due to suspected sensor icing. Ozone profiles from LTP are viewable at  
180 <[http://ozone.met.psu.edu/Panama\\_Data/index.html](http://ozone.met.psu.edu/Panama_Data/index.html)>. Each ozonesonde is calibrated  
181 according to standard procedures prior to launch; all LTP sondes were also compared to  
182 the TECO O<sub>3</sub> for 5-10 minutes pre-launch; agreement is within the stated precision of  
183 each technique (5%; Figure 1 in *Morris et al.*, 2010).

184 Ozone over Alajuela was measured by ENSCI ECC sondes with 1% KI with reduced  
185 (0.1%) buffer (**Table 1**); RS-80 radiosondes with a cryogenic frost-point hygrometer were  
186 used for P-T-U. At both ACR and LTP, most launches took place in early afternoon local  
187 time to capture Aura [*Schoeberl et al.*, 2006], Aqua and CALIPSO satellite overpasses

188 [Toon *et al.*, 2010]. Images and data for all Costa Rican (late 2005 start), Paramaribo  
189 (1999-present) and San Cristóbal (1999-present) ozonesonde and P-T-U profiles are  
190 available at <<http://croc.gsfc.nasa.gov/shadoz>> and at the World Ozone and Ultraviolet  
191 Data Centre, <<http://woudc.org>>.

192 Aircraft data used most often in analysis of the soundings are: O<sub>3</sub> from the  
193 FASTOZ *in-situ* instrument [Avery *et al.*, 2010], uv-DIAL and DACOM CO on the DC-8;  
194 the Cloud Physics Lidar (CPL) and Cloud Radar System (CRS) on the ER-2 [McGill *et al.*,  
195 2004; Hlavka *et al.*, 2010]. Regional cloud and convective information comes from  
196 meteorological analyses and GOES imagery, as archived by Toon *et al.* [2010].

### 197 2.3 Ancillary Data

198 As for IONS-04 [Thompson *et al.*, 2007a] and IONS-06 [Thompson *et al.*, 2008],  
199 tracers for O<sub>3</sub> origins include: (1) RH from the radiosonde P-T-U profiles; (2) Ertel's  
200 potential vorticity (pv; 1 pvu = 10<sup>-6</sup> m<sup>2</sup>s<sup>-1</sup>/K) computed from the Goddard Earth  
201 Observing System Assimilation Model (GEOS-version 4; Bloom *et al.*, 2005); (3) forward  
202 and backward air-parcel trajectories for each launch location and date, calculated with  
203 the kinematic version of the GSFC trajectory model [Schoeberl and Sparling, 1995] using  
204 GEOS meteorological fields at a 1x1-degree grid. Lightning imagery is also used to  
205 describe potential O<sub>3</sub> influences, as are absorbing aerosol data from OMI, trajectory-  
206 enhanced aerosol-exposure images and OMI NO<sub>2</sub> amounts. All back-trajectories in the  
207 TC4 region, aerosol and lightning data and trajectory-mapped exposure products are at  
208 the GSFC TC4 website: <<http://croc.gsfc.nasa.gov/tc4>>. In selected cases, additional  
209 trajectories were run with the NOAA Hysplit model (Draxler and Rolph, 2003).

### 210 2.4 Analysis for Wave Influences

211 In the LID (Laminar Identification; Thompson *et al.*, 2007a; 2008) technique, O<sub>3</sub>  
212 and potential temperature ( $\theta$ ) laminae, as described in Teitelbaum *et al.* [1994; 1996] and  
213 Pierce and Grant [1998] are used to identify RW and GW signatures as illustrated in  
214 **Figure 1**. The method is described as follows:

- 215 1) For each sounding, the O<sub>3</sub> and  $\theta$  laminae are isolated through normalization to  
216 running means. A boxcar smoothing over 2.5 km is used to isolate each lamina.  
217 Larger and smaller ranges (from 0.5 to 2.5 km) have been tested with little  
218 difference in laminar statistics. Normalized O<sub>3</sub> is the solid line in **Figure 1**; the  $\theta$   
219 deviations are signified by the dotted line. Because the ozone mixing ratio



220 precision is 5% in most of the region of interest, only laminae representing a  
221 deviation of  $\geq 10\%$  are included in the analysis (red vertical lines in **Figure 1**).

222 2): Correlations between  $O_3$  and  $\theta$  gradients are compared to identify GW and RW.  
223 Where the correlations (as in dashed line, **Figure 1**) exceed 0.7 GW (light green)  
224 is defined, based on the reasoning that such correlation between the two quantities  
225 signifies a vertical disturbance. Conversely, when horizontal motion affects  $O_3$ , it  
226 is poorly correlated with  $\theta$  and RW is specified. We adopt the practice of *Pierce*  
227 *and Grant* [1998] and *Teitelbaum et al.*, 1994], setting the RW limit for anti-  
228 correlation at  $\pm 0.3$ , corresponding to light blue sections in **Figure 1**. This is a  
229 fairly conservative criterion; see *Thompson et al.* [2007a] for sensitivity studies.

230 Two analyses are performed with the LID results. First, for an ensemble of soundings,  
231 wave frequencies at a given altitude are calculated from the percentage within a sample set  
232 that have laminae designated as RW or GW. Second, for each sounding, the contributions  
233 of RW and GW above the boundary layer (BL) to the tropopause or to 20 km are  
234 computed by integrating the amount of  $O_3$  within a given layer and adding up all the RW  
235 and GW segments. Thus, “tropospheric ozone” amounts in this paper are actually free  
236 tropospheric column amounts, above a BL top that varies from 1.2 km (San Cristóbal) to  
237 1.8 km (Paramaribo). The BL top is determined by taking the most negative second  
238 derivative of  $\theta$  with respect to altitude, between 0.4 and 2.5 km [*Yorks et al.*, 2009].  
239 Dobson Units (DU) are used; one DU =  $2.69 \times 10^{16} \text{ cm}^{-2}$ . The amount of  $O_3$  within the  
240 column not identified with RW or GW is labeled “other” in the budgets.

241 For determination of tropospheric LID  $O_3$  budgets (**Section 3**), an ozonopause  
242 definition of tropopause is employed (white dots, **Figure 2**; using the method of *Browell*  
243 *et al.*, 1996). This technique, in which  $O_3$  gradients are approached from the stratosphere,  
244 falls closer to the cold-point tropopause than the ozonopause of *Selkirk et al.* (2010; their  
245 Figure 2, from Alajuela soundings). *Thompson et al.* [2007a] showed that tropospheric  $O_3$   
246 columns can differ significantly under certain conditions, depending on the use of  $O_3$  or  
247 thermal tropopause. Such occurrences are infrequent in mid-latitudes ( $< 10\%$  in IONS-04  
248 or IONS-06 soundings) and are negligible in TC4, where *Selkirk et al.* (2010) showed that  
249 the thermal tropopause and chemical tropopause, based on either water vapor from frost-  
250 point hygrometry or  $O_3$  mixing ratios, was consistently at 350-355 K (147 hPa, 14.2 km);

251 the cold-point tropopause was always 370-378K (16-17 km). For a 1-2 km difference in  
252 thermal tropopause and the higher ozonopause, the O<sub>3</sub> budget might vary 2-3 DU.

### 253 **3. Results and Discussion: July-August 2007**

#### 254 **3.1. Overview of Ozone Profiles over LTP and ACR**

255 From time-series of O<sub>3</sub> mixing ratio over Las Tablas and Alajuela (**Figure 2**) the  
256 following features emerge: (1) Roughly 10% more O<sub>3</sub> is found in the LTP BL than at ACR  
257 due to pollution from Panamá City and occasionally from South American biomass fires.  
258 (2) The TTL extends lower over LTP than over ACR. It is customary to assume that when  
259 the free tropospheric segment of an ozone profile resembles BL concentrations that  
260 convective redistribution has taken place [Kley *et al.* 1996; Thompson *et al.*, 1997; Newell  
261 *et al.*, 1999, Folkins *et al.*, 2006]. Given typical BL concentrations of 20-25 ppbv at the  
262 two sites, **Figure 2** suggests that there are fewer episodes of high-altitude convection over  
263 LTP than ACR (blue shade, 12-14 km), although that inference may be an artifact of LTP  
264 having more samples. Consequently, there is less O<sub>3</sub> in the ACR mean O<sub>3</sub> profile between  
265 11-14 km (**Figure 3a**) than LTP (**Figure 3b**; cf Figure 13 in Avery *et al.*, 2010), giving a  
266 slight “S” shape in the ACR O<sub>3</sub> profile. The “S” is similar to Pacific SHADOZ profiles  
267 (Folkins *et al.*, 2000; 2006; cf Kley *et al.*, [1996]) and to IONS-06 soundings (<[http://  
268 croc.gsfc.nasa.gov/intexb/ionso6.html](http://croc.gsfc.nasa.gov/intexb/ionso6.html)>) over Mexico City (19N, 99W) that detected the  
269 highest O<sub>3</sub> at 8-9 km and minimum O<sub>3</sub> at 12-14 km (Thompson *et al.*, 2008; Fig 5).

270 Convective signatures in DC-8 sampling, registered as locally minimum ozone in  
271 profiles from the FASTOZ instrument, were concentrated between 10 and 11 km [Avery *et al.*  
272 *et al.*, 2010]. Elevated lower tropospheric tracers such as methyl hydrogen peroxide and  
273 organic bromine-containing constituents (Figures 13-15 in Avery *et al.*, 2010) occur  
274 coincidentally with the lower ozone. Mean DC-8 O<sub>3</sub> profiles and the soundings (**Figure**  
275 **3a**) are somewhat divergent. This is not surprising given that the sondes are at fixed  
276 locations whereas the DC-8 deliberately sampled in the vicinity of active convection.

#### 277 **3.2 Overview of Wave Signatures in the Sondes**

278 **Figure 4a** shows that the O<sub>3</sub> labeled GW is concentrated throughout the TTL and  
279 lower stratosphere over both LTP and ACR, with frequencies similar to those at the  
280 Paramaribo and San Cristóbal SHADOZ sites (**Figure 4b**). The latter depicts wave  
281 frequencies averaged for 1999-2007, which are nearly identical to June-July-August  
282 statistics. The waves in **Figures 4a,b** are similar to other SHADOZ tropical [Thompson  
283 *et al.*, 2010a,b] and northern hemisphere subtropical locations (Figure 4 in Thompson *et al.*  
284 *et al.*, 2008). As in Thompson *et al.* [2010a,b], the GW signal in the TTL is more frequent at

285 the station that is closer to the equator (Las Tablas and San Cristóbal, respectively, in  
286 | **Figures 4a** and **4b**). However, ACR has a higher GW frequency at 3 and 6 km, where  
287 | convective outflow often occurs (**Section 3.3**). Ozone associated with GW is 15-20% of  
288 | the tropospheric column (**Table 2**). In half the days with TC4 soundings at both LTP and  
289 | ACR, LTP O<sub>3</sub> at 3-6 km is 40-50 ppbv vs ~30 ppbv over ACR (cf **Figure 3** mean O<sub>3</sub>  
290 | profiles). Thus, column tropospheric O<sub>3</sub> is ~30% higher over LTP than ACR (**Table 2**).

### 291 | **3.3 Case Studies with Varying Convective and Wave Influence**

292 | Days with coincident launches at LTP and ACR (**Figure 5a**) offer an opportunity to  
293 | compare ozone profiles at the two sites and to use TC4 aircraft data, satellite imagery and  
294 | meteorological products to interpret convective and wave influences. On all dates  
295 | illustrated in **Figure 5a** the profiles display convective signatures typically with >10 DU  
296 | of column O<sub>3</sub> to 20 km designated as GW. The TC4 period started with a phase  
297 | characterized by active convection over the Costa Rica-Panamá region and the adjacent  
298 | Pacific (**Section 3.3.1**); this corresponds to the left-most section relative to the vertical  
299 | dashed line in **Figures 5b,c**. This is corroborated by satellite and aircraft imagery in  
300 | flights through 22 July 2007 [*Toon et al.*, 2010]. In a second phase, from 23 July through  
301 | 2 August (**Section 3.3.2**), between the two dashed lines in **Figures 5b,c**, TC4 aircraft  
302 | continued to sample convection but it was less active at ACR and LTP. The fraction of  
303 | total O<sub>3</sub> designated GW declined in most soundings (**Figures 5b,c**), as the GW-affected  
304 | segments in O<sub>3</sub> profiles retreated from the troposphere to above 17 km. The amount of  
305 | column O<sub>3</sub> affected by RW increased compared to the pre-24 July period. More active  
306 | convection resumed in a third phase (**Section 3.3.3**) after 2 August, when targeted  
307 | sampling by the ER-2, DC-8 and WB-57 took place [*Toon et al.*, 2010]. In the following  
308 | sections episodes illustrative of the three phases are examined to verify the link between  
309 | the GW designation and convective activity and the relationship of RW to extra-tropical  
310 | and/or pollution influences.

#### 311 | 3.3.1 13-22 July 2007: Active Convection and Elevated GW

312 | **13 July.** Convective activity at LTP and ACR, as given by GW amount to 20 km, is  
313 | similar (**Figure 5a**). The fraction of FT O<sub>3</sub> influenced by GW is similar in both cases  
314 | (~20%; **Figures 5b,c**). A typical pair of profiles (**Figure 6a**) shows that the ACR O<sub>3</sub>  
315 | concentration averages ~40 ppbv from the surface to the tropopause (14-15 km), whereas  
316 | O<sub>3</sub> in the upper troposphere over LTP exceeds 50 ppbv. BL O<sub>3</sub> at LTP is less than at ACR.  
317 | The RH profiles have considerable structure, with moister air over LTP than ACR.

318 Evidence for convection over ACR comes from the DC-8 flight from California to San Jose,  
319 Costa Rica, on 13 July 2007. The last 100-150 km of the flight encompassed a descent  
320 near ACR at ~2100 UTC, after the aircraft had crossed the ITCZ. The DC-8 uv-DIAL  
321 image of O<sub>3</sub> (**Figure 6b**) captures the morphology of convective impact throughout the FT  
322 and TTL. North of the ITCZ (northern edge at 13N), the FT was penetrated by pollution O<sub>3</sub>  
323 (>80 ppbv) and aerosols traced to biomass fires interacting with convection. South of the  
324 ITCZ, just before descent, FT O<sub>3</sub> dropped to 40-50 ppbv, except for a localized O<sub>3</sub>  
325 minimum (< 30 ppbv) around 10 km (**Figure 6b**), similar to FT O<sub>3</sub> structure over ACR  
326 (**Figure 6a**), and to the DC-8 FASTOZ O<sub>3</sub> during descent. Note a very thin layer of low  
327 ozone at 13 km in the uv-DIAL image, corresponding to an altitude with low O<sub>3</sub> over ACR.  
328 A similar low-O<sub>3</sub> “bubble” sampled on 17 July 2007 is discussed by *Petropavlovskikh et al.*,  
329 2010s. The uv-DIAL aerosols (not shown) corresponding to **Figure 6b** indicate a “clean”  
330 FT south of the ITCZ except for thin cirrus at the tropopause, consistent with the  
331 soundings. Convective indicators, elevated CO, methyl-hydrogen peroxide, lightning NO,  
332 ultrafine particles (not shown; see flight report at <<http://espo.nasa.gov/tc4/docs>>),  
333 penetrated south of the ITCZ. These pollutants came from north of the ITCZ.  
334 Interhemispheric transport during convection is well known over the Atlantic [*Jonquières*  
335 *et al.*, 1998; *Thompson et al.*, 2000; *Edwards et al.*, 2003].

336 On 13 July (**Figure 5b,c**) about half the tropospheric O<sub>3</sub> over both LTP and ACR  
337 corresponds to RW. The corresponding segments in the ACR profile (**Figure 6a**) are  
338 locally enhanced in O<sub>3</sub> and reduced in RH, suggesting extra-tropical influence. This is a  
339 good example of a sounding that captures both advective and convective signals.

340 **22 July.** On this day there is more O<sub>3</sub> in the TTL and LS identified as GW over  
341 LTP than ACR (**Figures 5a, 7a**). There is relatively little tropospheric O<sub>3</sub> associated with  
342 GW over either one (**Figures 5b,c**). A convective contrast between LTP and ACR is  
343 evident in satellite imagery (see ER-2 flight report for 22 July 07 at <[http://espo.](http://espo.nasa.gov/tc4/docs)  
344 [nasa.gov/tc4/docs](http://espo.nasa.gov/tc4/docs)>). When the ER-2 sampled near LTP on 22 July, the cloud and  
345 precipitation CPL-CRS imagery (**Figure 7b**) indicated several levels of convective  
346 outflow. For example, there is cirrus with a 13.5-14 km cloud top, coinciding with a GW-  
347 labeled segment in the LTP sounding, right above a localized O<sub>3</sub> minimum (black profile,  
348 **Figure 7a**). The CPL-CRS indicates another cloud outflow layer at 4 km. This region is  
349 not designated as GW although there is a local O<sub>3</sub> minimum at 4 km and relatively high  
350 RH. From 2-5 km the designation is RW; O<sub>3</sub> is 60% greater than at the surface, suggesting  
351 possible pollution transport. Surface ozone at LTP, measured in NATIVE on 22 July,

352 | averaged 15 ppbv (**Figure 8a**) but the moderately high CO mixing ratio, 135 ppbv,  
353 | supports an interpretation of pollution (**Figure 8b**).

### 354 | 3.3.2. 23 July-2 August: Elevated RW

355 | During the period 23-28 July most sonde launches were at LTP. At both sites, the  
356 | soundings from 23 July to 2 August displayed fractionally higher RW O<sub>3</sub> segments in the  
357 | troposphere (**Figure 5b,c**). An example appears in **Figure 9a**. The RW signal over LTP  
358 | extends from 2 to 17 km on 2 August, except for a 2-km region, and there is no GW  
359 | segment. ACR displays convective influence in terms of GW only from 11-15 km. An RW  
360 | segment from 5-10 km coincides with a dry layer from 4-9 km; this is suggestive of air  
361 | from the extra-tropics. Even though convection picks up on 3 August, remnants of the RW  
362 | feature persist over both sites on that day (**Figure 9b**).

363 | During the period of greater RW, there were also changes in surface O<sub>3</sub> and CO at  
364 | Las Tablas (see NATIVE data in **Figure 8**). On 23 July a normal diurnal O<sub>3</sub> cycle was  
365 | observed, with a near-zero nocturnal minimum. LID analysis for the 23 July sounding at  
366 | LTP was not valid, indicating active transition and no stable layers. However, on 24 July  
367 | the O<sub>3</sub> minimum rises to ~15 ppbv. This causes daily mean O<sub>3</sub> to increase from 17 ppbv on  
368 | 23 July to 25 ppbv on 24 July. At this time, CO dropped below 90 ppbv (**Figure 8b**), one  
369 | of the lowest values at NATIVE during TC4.

### 370 | 3.3.3 3-10 August: Return of Active Convection. Elevated GW

371 | **3 August.** The fractions of GW and RW tropospheric segments over Las Tablas  
372 | and Alajuela are nearly the same (**Figures 5b,c**) and the wave structures are similar  
373 | (**Figure 9b**). Over LTP the GW signal that was absent on 2 August returns at 13-20 km  
374 | (**Figure 9b**). The DC-8 and ER-2 sampled not far from LTP near active convection (refer  
375 | to GOES image with flight tracks for all three aircraft on 3 August; Figure 16 in *Toon et al.*  
376 | [2010]). The DC-8 profiles in **Figure 10a** were taken over NATIVE from 1705-1735 UTC  
377 | during the convective period that was sampled less than 50 km away by the ER-2; the LTP  
378 | launch took place at 1741 UTC. The upper of two O<sub>3</sub> minima over LTP (10-15 km, **Figure**  
379 | **9b**), corresponds to cloud outflow recorded by satellite imagery (not shown) and to cirrus  
380 | in the ER-2 CPL-CRS product (**Figure 10b**) at 13-15 km. A second O<sub>3</sub> minimum with  
381 | elevated CO at 5-6 km (**Figure 10a**) is also located at a cloud outflow layer (lower **bar**  
382 | arrow in **Figure 10b**). Over ACR, O<sub>3</sub> mixing ratios averaged > 80 ppbv in the 6-13 km  
383 | segment (**Figure 9b**). Above 8 km, the RH drops off sharply, suggesting extra-tropical  
384 | air. The elevated O<sub>3</sub> coincides with a mostly RW segment that brackets the tropopause,  
385 | which is 1.5 km higher over LTP than ACR (**Figure 2**).

386 **5 August.** During the period 3-5 August there was a sharp transition in the LTP  
387 and ACR profiles that is reflected in the O<sub>3</sub> budgets (**Figures 5a-c**); the GW O<sub>3</sub> budgets to  
388 20 km are nearly identical over the two stations on 4 August (**Figure 5a**). The upper  
389 tropospheric O<sub>3</sub> mixing ratios decline over both sites, from a mean of ~75 ppbv on 3  
390 August to 45 ppbv on 5 August (**Figures 9b,c**); during the transition, LTP free  
391 tropospheric O<sub>3</sub> declines to 22 DU on 4 August, the lowest O<sub>3</sub> column in the TC4 period  
392 (**Figure 5b**). From 4 to 5 August there are further transitions in vertical O<sub>3</sub> structures  
393 over ACR and LTP (**Figure 9c**). The GW signal that starts over LTP (ACR) at 12 km (11  
394 km) on 4 August (not shown) retreats to 15 km on 5 August. Over Las Tablas a several-km  
395 thick layer that is 20 ppbv above background coincides with RW (**Figure 9c**; also **Figure**  
396 **1**). DC-8 aircraft sampling near LTP on 5 August confirmed the possibility of extra-  
397 tropical origins at 8-10 km, where O<sub>3</sub> mixing ratios were 50-70 ppbv in a relatively dry  
398 layer [Avery *et al.*, 2010]. However, just above this layer, at 11 km, the DC-8 noted cleaner  
399 than usual conditions, signifying convective outflow of marine boundary layer air (upper  
400 outflow on **Figure 10c**). Near the surface, the DC-8 detected pollution due to biomass  
401 fires (Flight notes at <<http://www.espo.nasa.gov/tc4/flightDocs.php>>).

402 The 5 August ozonesonde launch at LTP (1505 UTC) was timed for nearby DC-8  
403 spiral (~1540 UTC) and ER-2 sampling of convective cells to the southwest (**Figure 10c**;  
404 cf Figure 19 in Toon *et al.*, 2010). Between 2.5 km and 5.1 km, the sonde bounced up and  
405 down five times within a convective cell while O<sub>3</sub> concentrations increased by ~10 ppbv.  
406 Morris *et al.* [2010] use satellite imagery, lightning data, radar and OMI NO<sub>2</sub> maps, along  
407 with DC-8 measurements to demonstrate that lightning NO production is responsible for  
408 much of the increase. The lower outflows in **Figure 10c** correspond to the region of the  
409 bouncing sonde. The profile in **Figure 9c** is based on the final sonde ascent from 2.5 to  
410 5.1 km; the GW signal is not detected.

#### 411 **4. Waves in the Equatorial Americas: 1999-2007. TC4 in Context.**

412 A perspective for interpreting convective influence over LTP and ACR is provided  
413 by wave frequencies over Paramaribo and San Cristóbal (**Figure 4b**), SHADOZ sites  
414 operating since 1999 [Thompson *et al.*, 2003a,b]. The amplitudes of individual layers and  
415 wave structure at Paramaribo and San Cristóbal resemble those for LTP and ACR (**Figure**  
416 **1**) as do the structure of the GW frequencies at LTP and ACR (**Figures 4a,b**). Similar GW  
417 structure appears over equatorial Indian Ocean sites, eg Watukosek, Kuala Lumpur, that  
418 display the highest annually averaged GW frequency, ~60% [Thompson *et al.*, 2010a].  
419 The higher GW frequency at San Cristóbal leads to a larger GW fraction of tropospheric O<sub>3</sub>

420 | (**Figure 11**). Although the tropospheric O<sub>3</sub> column averaged 25 DU in 2007, compared to  
421 | 28 DU for LTP, 25% of O<sub>3</sub> is GW-affected at San Cristóbal compared to 15% at LTP (**Table**  
422 | **2**). TC4 was timed for the onset of the sub-tropical convective season and the North  
423 | American monsoon. **Figure 4c**, a summary of monthly averaged GW over Paramaribo,  
424 | shows that JJA has about half the maximum GW frequency, typically a December  
425 | occurrence.

426 | An interannual view of ozone budgets and convective influence appears in **Figure**  
427 | **11**, where the mean JJA tropospheric O<sub>3</sub> column (with segments for RW and GW) is  
428 | displayed for Costa Rica (2006 only), Paramaribo and San Cristóbal from 1999-2007. At  
429 | San Cristóbal, 2006 is a low-O<sub>3</sub> year compared to the six others, possibly due to a  
430 | moderate El Niño [Arguez, 2007]. In the eastern Pacific, El Niño tends to enhance  
431 | convective activity, mixing lower O<sub>3</sub> air from the BL throughout the troposphere. [Logan  
432 | *et al.*, 2008]. The GW-affected tropospheric ozone amount in 2006 is only slightly lower  
433 | than normal over San Cristóbal but the total tropospheric column dropped from a mean  
434 | 22-23 DU (1999-2005; **Figure 11**) to 18 DU so the GW fraction is magnified. At Heredia  
435 | (20 km away) 2006 tropospheric O<sub>3</sub> is lower than over ACR in 2007 (**Figure 11**).

436 | General meteorological conditions at Paramaribo (6N), Panamá (8N), and Alajuela  
437 | (10N) are similar, with the ITCZ migrating over each. The SHADOZ wave climatology  
438 | [Loucks, 2007; Thompson *et al.*, 2010] shows GW frequency diminishing with increasing  
439 | latitude. A GWI (Gravity Wave Index; **Figure 12**), based on the fraction of the O<sub>3</sub> column  
440 | to 20 km denoted as GW, provides a quantitative comparison of site-to-site and  
441 | interannual variability. GWI is larger at San Cristóbal than Paramaribo until 2004 when  
442 | data gaps at San Cristóbal compromise the record. The gaps also preclude conclusive  
443 | linkage of GWI to signals associated with an El Niño.

## 444 | **5. Summary**

445 | During TC4, in July and early August 2007, ozonesondes and radiosondes were  
446 | launched several times/week at Alajuela, Costa Rica (10N,84W) to characterize convective  
447 | influences in the tropical tropopause layer (TTL). At Las Tablas, Panamá (7.8N, 80W), a  
448 | coastal site 300 km southwest of Panamá City, O<sub>3</sub> profiles from daily sondes, surface O<sub>3</sub>,  
449 | CO and other tracers are analyzed. Laminar identification provides a systematic approach  
450 | to classifying wave signatures in sounding data, giving a statistical perspective on the TC4  
451 | period and the longer-term SHADOZ sounding record at Paramaribo and San Cristóbal.  
452 | The findings are summarized:

- GW influences, possibly due to semi-permanent Kelvin waves in the TTL and lower stratosphere (cf *Grant et al.*, 1998; *Thompson et al.*, 2010a) appeared in 50% (40%) of Las Tablas (Alajuela) sondes. The GW structure and frequency are similar to those over SHADOZ stations at San Cristóbal and Paramaribo.
- On average there is 35-40% more tropospheric column O<sub>3</sub> at LTP than ACR during TC4 and 20% more at LTP than at San Cristóbal, a remote marine station, 1400 km southwest of LTP.
- June-July-August O<sub>3</sub> budgets at Paramaribo and San Cristóbal suggest that 2007 was a “typical” year in terms of tropical equatorial O<sub>3</sub> amount and convective activity expressed in GW frequency. During 1999-2006, Paramaribo and San Cristóbal display O<sub>3</sub> column amounts and convective influence that bracket the TC4 ACR and LTP values.

Classification of wave types through LID is validated through case studies in which aircraft observations support interpretation of convective influences (with the GW designation) and extra-tropical impact, corresponding to RW. Laminae of low-O<sub>3</sub> surface air convectively injected into the free troposphere are detected by LID, frequently interleaved with the richer-O<sub>3</sub> layers; subtle day-to-day variations are captured. The pattern of convection inferred from LID is consistent with the meteorological evolution of the campaign [*Toon et al.*, 2010]. The early part of TC4, to 22 July 2007, was characterized by persistent GW throughout the free troposphere and TTL. After a less active period, from 23 July until approximately 2 August, with lower GW signals and greater RW, GW increased in frequency along with convection.

Sonde and aircraft data established further the convection-GW linkage and demonstrated the prevalence of extra-tropical laminae interleaved with layers from convective outflow throughout the equatorial Americas. In terms of TC4 objectives, our analysis of ozone structure strengthens the case for convection as a dominant mechanism for water vapor transport and cirrus formation in the TTL. The persistence of higher-O<sub>3</sub> laminae in the troposphere requires further investigation to determine the extent to which these layers are remnants of extra-tropical filaments or associated with localized equatorial waves.

Acknowledgments. We are grateful to NASA’s Upper Air Research Program and Aura Validation (M. J. Kurylo; K. W. Jucks) that sponsored the Las Tablas and Alajuela TC4 soundings and ground-based measurements at Las Tablas. These programs, with NOAA support, also sponsor SHADOZ at Costa Rica and San Cristóbal. The Paramaribo station is sponsored by KNMI and the Suriname Meteorological Department. Additional analysis support came from NASA’s Tropospheric Chemistry Program (J. H.



488 Crawford, J. A Al-Saadi). Las Tablas measurements with the NATIVE trailer were assisted by A. Pino and  
 489 L. Jordan (University of Panamá); A. M. Bryan and D. Lutz (Valparaiso Univ); Z. Chen and J. L. Tharp  
 490 (PSU). Costa Rican launches were made by UNA students K. Cerna, V. H. Beita, D. Gonzalez. Thanks to  
 491 Mission Scientists M. R. Schoeberl and P. A. Newman for flight notes and to K. E. Pickering for  
 492 discussing lightning data. Thanks to EAB, BvdW, AOG (PSU) for analysis.

493 **APPENDIX. ABBREVIATIONS AND ACRONYMS**

494 ACP= Alajuela, Costa Rica (10N, 84W)  
 495 BL = Boundary Layer, here determined from radiosondes (*Yorks et al.* 2009)  
 496 CALIPSO = Cloud-Aerosol Lidar and Infrared Pathfinder Satellite Observation  
 497 CPL = Cloud Physics Lidar (ER-2 instrument)  
 498 CRS = Cloud Radar System (ER-2 instrument)  
 499 DU = Dobson Unit (1 DU =  $2.69 \times 10^{16} \text{ cm}^{-2}$ )  
 500 ECC = Electrochemical Concentration Cell (ozonesonde type)  
 501 FT = Free Troposphere  
 502 GOES = Geostationary Operational Environmental Satellites  
 503 GSFC = Goddard Space Flight Center  
 504 GWI = Gravity Wave Index  
 505 INTEX = Intercontinental Transport Experiment (-A, 2004; B, 2006)  
 506 IONS = INTEX Ozonesonde Network Study <<http://croc.gsfc.nasa.gov/intex/ions.html>; ...  
 507 intexb/ionso6>  
 508 ITCZ = Intertropical Convergence Zone  
 509 JJA = June-July-August  
 510 LTP = Las Tablas, Panamá (7.8N, 80W)  
 511 NASA = National Aeronautics and Space Administration  
 512 OMI = Ozone Monitoring Instrument  
 513 P-T-U = Pressure-Temperature-Humidity  
 514 RH = Relative Humidity  
 515 RWI = Rossby Wave Index  
 516 SHADOZ = Southern Hemisphere Additional Ozonesondes  
 517 <<http://croc.gsfc.nasa.gov/shadoz>>  
 518 SOWER = Stratospheric Ozone and Water Vapor in Equatorial Regions  
 519 TC4 = Tropical Composition, Clouds and Climate Coupling (2007)  
 520 <<http://espo.nasa.gov/tc4>>  
 521 TCSP = Tropical Convective Systems and Processes (Costa Rica, 2005)  
 522 TTL = Tropical Tropopause Layer (sometimes tropopause transition layer)  
 523 UV-DIAL = Ultraviolet Differential Airborne Lidar [Laser Detection and Ranging]

524 **Table 1.** Stations for which data are used. Further technical details given in Table A-1 in  
 525 *Thompson et al.* (2003a) and in *Thompson et al.* (2007b).

526 Station	527 Latitude, Longitude	528 Instrument Type	529 Sensing Solution	530 Radiosonde	531 Co-Investigator/ 532 Sponsor
528 Las Tablas	7.8N, 80W	529 ENSCI, 0.5% KI, buffered	530 RS-80-15N	531 G. A. Morris, A. M. Thompson	
529 Heredia/Alajuela,	10.0N, 84 W	530 ENSCI, 1% KI, buffered	531 RS-80& Cryogenic Frost-point hygrometer	532 H. Vömel; J. Valverde Canossa	
531 San Cristóbal	0.92S, 89.6W	532 ENSCI 2% unbuffered	533 RS-80	534 H. Vömel. INAMHI (National	
532		533 to 2006; 1%, reduced		534 Inst. of Hydrology and	
533		534 buffer, 2006-		535 Meteorology of Ecuador), M. V. A.	
534				536 Reyes [ <i>Johnson et al.</i> , 2002; <i>Thompson</i>	
535				537 <i>et al.</i> , 2007b]	
536 Paramaribo	5.8N, 55W	537 SPC, 1% KI buffered	538 RS-80 to 2005	539 G. Verver & Met. Service	
537			540 RS-92, 2005-	541 Suriname [ <i>Peters et al.</i> ,	
538				542 2003; <i>Fortuin et al.</i> , 2006]	

**Table 2.** Free tropospheric ozone columns during June-July-August 2007. ACR mean omits 28 July sounding where data ended below the tropopause.

Station	GW O <sub>3</sub>	RW O <sub>3</sub>	Other O <sub>3</sub>	Total
ACR - DU	2.9	8.2	9.3	20.4
ACR - %	14	40	46	100
LTP - DU	3.94	13.2	10.8	28
LTP - %	15	47	38	100
San Cris.- DU	5.5	7.5	12	25
San Cris.- %	24	28	48	100

## References

- Arguez, A., ed. (2007): State of the climate in 2006. *Bull. Am. Meteor. Soc*, **88**, S1-S135.
- Avery, M. A., J. Joiner, C. Twohy, D. McCabe, E. Atlas, D. Blake, P. Bui, J. Counse, J. Dibb, G. Diskin, R. Gao, P. Lawson, M. McGill, D. Rogers, G. Sachse, R. Salawitch, E. Scheuer, K. Severance, A. M. Thompson, C. Trepte, P. Wennberg, J. Ziemke, (2010) Convective distribution of tropospheric ozone and tracers in the central American ITCZ Region: Evidence from observations during TC4, *J. Geophys. Res.*, doi: 10.1029/2009JD013450, in press. Manuscript available at TC4 website. Contact [btoon@lasp.colorado.edu](mailto:btoon@lasp.colorado.edu) for password.
- Bertram, T., et al. (2007), Direct measurements of the convective recycling of the upper troposphere, *Science*, **315**, 816–820, doi:10.1126/science.1134548.
- Bloom, S., et al. (2005), Documentation and validation of the Goddard Earth Observing System (GEOS) data assimilation system - Version 4. Technical Report Series on Global Modeling and Data Assimilation 104606.
- Browell, E. V., et al. (1996), Ozone and aerosol distributions and air mass characteristics over the South Atlantic Basin during the burning season, *J. Geophys. Res.*, **101**, 24,043-24,068.
- Cooper, O. R., et al. (2006), Large upper tropospheric ozone enhancements above mid-latitude North America during summer: In situ evidence from the IONS and MOZAIC ozone networks, *J. Geophys. Res.*, **111**, D24S05, doi: 10.1029/2006JD007306.
- Deshler, T., et al. (2008), Balloon experiment to test ECC-ozonesondes from different manufacturers, and with different cathode solution strengths: Results of the BESOS flight, *J. Geophys. Res.*, **113**, D04307, doi:10.1029/2007JD008975.
- Dougherty, K. M. (2008), The effect of ozonopause placement on tropospheric ozone budgets: An analysis of ozonesonde profiles from selected IONS-06 sites, MS Thesis, The Pennsylvania State University.
- Draxler, R. R., and G. D. Rolph (2003), HYSPLIT (Hybrid Single-Particle Lagrangian Integrated Trajectory) model, <http://www.arl.noaa.gov/ready/hysplit4.html>, NOAA Air Resour. Lab., Silver Spring, MD.
- Edwards, D. P., et al. (2003), Tropospheric ozone over the tropical Atlantic: A satellite perspective, *J. Geophys. Res.*, **108**, 4237, doi: 10.1029/2002JD002927.
- Fast, J. D., et al. (2007), A meteorological overview of the MILAGRO field campaign, *Atmos. Chem. Phys.*, **7**, 2233-2257.
- Folkens, I., S. J. Oltmans, and A. M. Thompson (2000), Tropical convective outflow and near-surface equivalent potential temperatures, *Geophys. Res. Lett.*, **27**, 2549-2552.

- 584 Folkins, I., P. Bernath, C. Boone, K. Walker, A. M. Thompson, and J. C. Witte (2006), The  
585 seasonal cycles of O<sub>3</sub>, CO and convective outflow at the tropical tropopause, *Geophys.*  
586 *Res. Lett.*, **33**, L16802, doi:10.1029/2006GLO26602.
- 587 Fortuin, P., et al. (2007), Origin and transport of tropical cirrus clouds observed over  
588 Paramaribo, Suriname (5.8°N, 55.2°W), *J. Geophys. Res.*, **112**, D09107,  
589 doi:10.1029/2005JD006420.
- 590 Fueglistaler, S., A. E. Dessler, T. J. Dunkerton, I. Folkins, Q. Fu, and P. W. Mote (2009),  
591 Tropical tropopause layer, *Rev. Geophys.*, **47**, RG1004, doi:10.1029/2008RG000267.
- 592 Fujiwara, M., K. Kita, and T. Ogawa (1998), Stratosphere-troposphere exchange of ozone  
593 associated with the equatorial Kelvin wave as observed with ozonesondes and  
594 rawinsondes, *J. Geophys. Res.*, **103**, No. D15, 19,173-19,182.
- 595 Fujiwara, M., F. Hasebe, M. Shiotani, N. Nishi, H. Vömel, and S. J. Oltmans (2001), Water  
596 vapor control at the tropopause by equatorial Kelvin waves observed over the  
597 Galápagos, *J. Geophys. Res.*, **28**, 3143-3146.
- 598 Grant, W. B., R. B. Pierce, S. J. Oltmans, and E. V. Browell (1998), Seasonal evolution of total  
599 and gravity wave induced laminae in ozonesonde data in the tropics and subtropics,  
600 *Geophys. Res. Lett.* **25**, 1863-1866.
- 601 Hasebe, F., M. Fujiwara, N. Nishi, M. Shiotani, H. Vömel, S. Oltmans, H. Takashima, S.  
602 Saraspriya, N. Komala, and Y. Inai (2007), In situ observations of dehydrated air  
603 parcels advected horizontally in the Tropical Tropopause Layer of the western Pacific,  
604 *Atmos. Chem. Phys.*, **7**, 803-813.
- 605 Hlavka, D., L. Tian, W. Hart, L. Li, M. McGill, and G. Heymsfield (2010), Vertical cloud  
606 climatology during TC4 derived from high-altitude aircraft merged lidar and radar, *J.*  
607 *Geophys. Res.*, this issue.
- 608 Johnson, B. J., S. J. Oltmans, H. Vömel, T. Deshler, C. Kroger, and H. G. J. Smit (2002), ECC  
609 ozonesondes pump efficiency measurements and sensitivity tests of buffered and  
610 unbuffered sensor solutions, *J. Geophys. Res.*, *107*(D19), 4393, doi:  
611 10.1029/2001JD000557.
- 612 Jonquière, I., A. Marenco, A. Maalej, and F. Rohrer (1998), Study of ozone formation and  
613 transatlantic transport from biomass burning emissions over West Africa during the  
614 airborne Tropospheric Ozone Campaigns TROPOZ I and TROPOZ II, *J. Geophys. Res.*,  
615 **103**, 19,059–19,073.
- 616 Kley, D., P. J. Crutzen, H. G. J. Smit, H. Vömel, S. J. Oltmans, H. Grassl and V. Ramanathan  
617 (1996) Observations of near-zero ozone over the convective Pacific: Effects on air  
618 chemistry, *Science*, **274**, 230-233.
- 619 Logan, J. A., I. Megretskaya, R. Nassar, L.T. Murray, L. Zhang, K.W. Bowman, H.M. Worden,  
620 and M. Luo (2008), Effects of the 2006 El Nino on tropospheric composition as  
621 revealed by data from the TES, *Geophys. Res. Lett.*, **35**, L03816,  
622 doi:10.1029/2007GLO31698.
- 623 Loucks, A. L. (2007), Evaluation of dynamical sources of ozone laminae in the tropical  
624 troposphere and tropical tropopause layer, M.S. Thesis, Penn State University.
- 625 McGill, M. J., L. Li, W. D. Hart, G. M. Heymsfield, D. L. Hlavka, P. E. Racette, L. Tian, M. A.  
626 Vaughan, and D. M. Winker (2004), Combined lidar-radar remote sensing: Initial  
627 results from CRYSTAL-FACE, *J. Geophys. Res.*, **109**, D07203,  
628 doi:10.1029/2003JD004030.
- 629 Morris, G. A., et al. (2010), Observations of ozone production in a dissipating convective cell  
630 during TC4, *J. Geophys. Res.*, doi: 10.1029/2009JD 014098, submitted. Manuscript  
631 available at TC4 website. Contact [btoon@lasp.colorado.edu](mailto:btoon@lasp.colorado.edu) for password.
- 632 Newell, R. N., V. Thouret, J. Y. N. Cho, P. Stoller, A. Marenco, and H. G. Smit (1999), Ubiquity  
633 of quasi-horizontal layers in the troposphere, *Nature*, **398**, 316-319.
- 634 Oltmans, S.J., et al. (2001), Ozone in the Pacific tropical troposphere from ozonesonde  
635 observations, *J. Geophys. Res.*, **106**, 32503-32526.

- 636 Oltmans, S. J., et al. (2004), Tropospheric ozone over the North Pacific from ozonesonde  
637 observations, *J. Geophys. Res.*, **109**, D15S01, doi: 10.1029/2003JD003466.
- 638 Peters, W., P. Fortuin, H. Kelder, C.R. Becker, J. Lelieveld, P.J. Crutzen, and A.M. Thompson  
639 (2004), Tropospheric ozone over a tropical Atlantic station in the Northern  
640 Hemisphere: Paramaribo, Surinam (6°N, 55°W), *Tellus*, **56**, 21-34.
- 641 Petropavloskikh, I., E. Ray, S. M. Davis, K. Rosenlof, G. Manney, R. Shetter, S. Hall, K.  
642 Ullmann, L. Pfister, J. Hair, M. Fenn, M. Avery, and A. M. Thompson, (2010) Low ozone  
643 bubbles observed in the tropical tropopause layer during the TC4 campaign in 2007, *J.*  
644 *Geophys. Res.*, doi: 10.1029/2009JD012804, in press. Manuscript available at TC4  
645 website. Contact [btoon@lasp.colorado.edu](mailto:btoon@lasp.colorado.edu) for password.
- 646 Pierce, R. B., and W.B. Grant (1998), Seasonal evolution of Rossby and gravity wave induced  
647 laminae in ozonesonde data obtained from Wallops Island, Virginia, *Geophys. Res.*  
648 *Lett.*, **25**, 1859-1862.
- 649 Piotrowicz, S. R., H. Bezdek, G. Harvey, and M. Springer-Young (1991), On the ozone minimum  
650 over the equatorial Pacific Ocean. *J. Geophys. Res.* **96**, 18679-18687.
- 651 Randel, W. J., D. J. Seidel, and L. L. Pan (2007), Observational characteristics of double  
652 tropopauses, *J. Geophys. Res.*, **112**, D07309, doi:10.1029/2006JD007904.
- 653 Randriambelo, T., J-L. Baray, S. Baldy, A. M. Thompson, S. J. Oltmans, and P. Keckhut (2003),  
654 Investigation of the short-term variability of tropical tropospheric ozone, *Annales*  
655 *Geophysiques*, **21**, 2095-2106.
- 656 Read, K. A. et al. (2008), Extensive halogen-mediated ozone destruction over the tropical  
657 Atlantic Ocean, *Nature*, **453**, 1232-1235, doi: 10.1038/nature07035.
- 658 Schoeberl, M. R., and L.C. Sparling (1995), Trajectory modeling: Diagnostic tools in  
659 atmospheric physics, S. I. F. Course CXVI, edited by G. Fiocco and C. Visconti, North-  
660 Holland, Amsterdam.
- 661 Schoeberl, M. R., et al. (2006), Overview of the EOS aura mission, *IEEE Trans.*, **44** (5), 1066-  
662 1074, doi:10.1109/TGRS.2005.861950.
- 663 Selkirk, H. B., H. Vömel, J. M. Valverde Canossa, L. Pfister, J. A. Diaz, W. Fernández, J.  
664 Amador, W. Stolz, and G. Peng, The detailed structure of the tropical upper troposphere  
665 and lower stratosphere as revealed by balloonsonde observations of water vapor, ozone,  
666 temperature and winds during the NASA TCSP and TC4 Campaigns, *J. Geophys. Res.*,  
667 in press. \*\* Manuscript available at TC4 website. Contact [btoon@lasp.colorado.edu](mailto:btoon@lasp.colorado.edu) for  
668 password.
- 669 Smit, H. G. J., et al. (2007), Assessment of the performance of ECC-ozonesondes under quasi-  
670 flight conditions in the environmental simulation chamber: Insights from the Jülich  
671 Ozone Sonde Intercomparison Experiment (JOSIE), *J. Geophys. Res.*, **112**, D19306, doi:  
672 10.1029/2006JD007308.
- 673 Takashima, H., and M. Shiotani (2007), Ozone variation in the tropical tropopause layer as  
674 seen from ozonesonde data, *J. Geophys. Res.*, **112**, D11123,  
675 doi:10.1029/2006JD008322.
- 676 Teitelbaum, H., J. Ovarlez, H. Kelder, and F. Lott (1994), Some observations of gravity-wave-  
677 induced structure in ozone and water vapour during EASOE, *Geophys. Res. Lett.*, **21**,  
678 1483-1486.
- 679 Teitelbaum, H., et al. (1996), The role of atmospheric waves in the laminated structure of ozone  
680 profiles at high latitude. *Tellus*, **48A**, 442-455.
- 681 Thompson, A. M., et al. (1993), SAGA-3 ozone observations and a photochemical model  
682 analysis of the marine boundary layer during SAGA-3, *J. Geophys. Res.*, **98**, 16955-  
683 16968.
- 684 Thompson, A. M., et al. (1996), Where did tropospheric ozone over southern Africa and the  
685 tropical Atlantic come from in October 1992? Insights from TOMS, GTE/TRACE-A and  
686 SAFARI-92, *J. Geophys. Res.*, **101**, 24,251-24,278.
- 687 Thompson, A. M., W.-K. Tao, K. E. Pickering, J. R. Scala, and J. Simpson (1997), Tropical deep  
688 convection and ozone formation, *Bull. Amer. Met. Soc.*, **78**, 1,043-1,054.

- 689 Thompson, A. M., B. G. Doddridge, J. C. Witte, R. D. Hudson, W. T. Luke, J. E. Johnson, B. J.  
690 Johnson, S. J. Oltmans, and R. Weller (2000), A tropical Atlantic paradox: Shipboard  
691 and satellite views of a tropospheric ozone maximum and wave-one in January-  
692 February 1999, *Geophys. Res. Lett.*, **27**,3317-3320.
- 693 Thompson, A. M., et al. (2003a), Southern Hemisphere Additional Ozonesondes (SHADOZ)  
694 1998-2000 tropical ozone climatology. 1. Comparison with TOMS and ground-based  
695 measurements, *J. Geophys. Res.*, **108**, 8238, doi: 10.1029/2001JD000967.
- 696 Thompson, A. M., et al. (2003b), Southern Hemisphere Additional Ozonesondes (SHADOZ)  
697 1998-2000 tropical ozone climatology. 2. Tropospheric variability and the zonal wave-  
698 one, *J. Geophys. Res.*, **108**, 8241, doi: 10.1029/2002JD002241.
- 699 Thompson, A. M., et al. (2007a), IONS (INTEX Ozone Sonde Network Study, 2004). 1.  
700 Summertime UT/LS (Upper Troposphere/Lower Stratosphere) ozone over northeastern  
701 North America, *J. Geophys. Res.*, **112**, D12S12, doi: 10.1029/2006JD007441.
- 702 Thompson, A. M., J. C. Witte, H. G. J. Smit, S. J. Oltmans, B. J. Johnson, V. W. J. H. Kirchhoff,  
703 and F. J. Schmidlin (2007b), Southern Hemisphere Additional Ozonesondes (SHADOZ)  
704 1998-2004 tropical ozone climatology. 3. Instrumentation, station variability,  
705 evaluation with simulated flight profiles, *J. Geophys. Res.*, **112**, D03304, doi: 10.1029/  
706 2005JD007042.
- 707 Thompson, A. M., J. E. Yorks, S. K. Miller, J. C. Witte, K. M. Dougherty, G. A. Morris, D.  
708 Baumgardner, L. Ladino, and B. Rappenglueck (2008), Tropospheric ozone sources and  
709 wave activity over Mexico City and Houston during Milagro/Intercontinental Transport  
710 Experiment (INTEX-B) Ozone Sonde Network Study, 2006 (IONS-06), *Atmos. Chem.*  
711 *Phys.*, **8**, 5113-5125.
- 712 Thompson, A. M., A. L. Loucks, S. Lee, S. K. Miller (2010a), Gravity and Rossby wave  
713 influences in the tropical troposphere and lower stratosphere based on SHADOZ  
714 (Southern Hemisphere Additional Ozonesondes) soundings, 1998-2007, *J. Geophys.*  
715 *Res.*, doi: 10.1029/2009JD013429, submitted.
- 716 Thompson, A. M., S. J. Oltmans, D. W. Tarasick, P. Von der Gathen, H. G. J. Smit, J. C. Witte  
717 (2010b), Strategic ozone sounding networks: Review of design and accomplishments,  
718 *Atmos. Environ.*, in press.
- 719 Toon, O. B., et al. (2010), Planning and implementation of the Tropical Composition, Cloud and  
720 Climate Coupling Experiment (TC4), *J. Geophys. Res.*, this issue. Manuscript available  
721 at TC4 website. Contact [btoon@lasp.colorado.edu](mailto:btoon@lasp.colorado.edu) for password.
- 722 Torres, A. L., and A. M. Thompson (1993), Nitric oxide in the equatorial Pacific boundary layer:  
723 SAGA-3 measurements, *J. Geophys. Res.*, **98**, 16949-16954.
- 724 Yorks, J. E., A. M. Thompson, E. Joseph, and S. K. Miller (2009), The variability of free  
725 tropospheric ozone over Beltsville, Maryland (39N, 77W) in the summers 2004-2007,  
726 *Atmos. Environ.*, **43**, 1827-1838.
- 727 Zafiriou, O. C., M. McFarland, and R. H. Bromund (1980) Nitric oxide in seawater,  
728 *Science*, **207**, 637-639, 1980.

FIGURE CAPTIONS -

Fig 1

Application of laminar identification (LID) method to typical sounding from Panamá. Illustrated are normalized  $O_3$  (solid line), potential temperature (dotted line) and correlation between the two quantities (dashed). Correlation criteria for Rossby waves (RW) are within vertical lines between -0.3 and +0.3 (light blue). The latter designation is used in discussion of profiles and budgets. Gravity wave (GW) criterion of *Pierce and Grant* (1998; see their Figure 1) and *Thompson et al.* (2007a; Figure 3) calls for normalized  $O_3$  and  $\theta$  correlation to reach 0.7 (vertical line; light green for budgets). For

computation of the GW Index, a more restrictive criterion is used, namely, the corresponding  $O_3$  layer amplitude must exceed 0.1 (10%), as in the darker green. An RW Index, not used here, is based on counting only ozone within dark blue.

Fig 2 Curtain plots of  $O_3$  mixing ratio to 18 km during TC4 over (a) Alajuela, Costa Rica (ACR); (b) Las Tablas, Panamá (LTP). White dots refer to the ozonopause as described in the text.

Fig 3 Mean profiles of ozone, temperature, relative humidity (RH) from surface to 20 km for: (a) Alajuela, Costa Rica (ACR); eight  $O_3$  profiles with slight interference from volcanic  $SO_2$  have been smoothed at 3 km. For comparison, mean DC-8 profiles from the FASTOZ ozone instrument (green dots) are displayed. The profiles include landing and takeoffs from San Jose airport near Alajuela. (b) Las Tablas, Panamá. In the latter case, seven questionable RH profile segments are omitted from mean.

Fig 4 (a) Frequency of GW occurrence over LTP, ACR during July-August 2007 TC4 sampling; (b) mean GW frequency over Paramaribo and San Cristóbal, based on all 1999-2007 profiles. For (b) J-J-A and full year means are virtually the same because J-J-A frequencies fall about halfway between the annual maximum and minimum frequencies. Paramaribo did not launch during TC4; (c) annual GW frequency at Paramaribo. The latter is typical of near-equatorial SHADOZ sites [Thompson *et al.*, 2010a].

Fig 5 (a) Amounts of  $O_3$  (in DU) from top of the BL to 20 km, affected by GW, RW determined by LID [Thompson *et al.*, 2007a] based on  $O_3$  and P-T-U soundings from days with both Las Tablas (LTP) and Alajuela (ACR) launches during TC4. (b) Same as (a) except for free tropospheric  $O_3$  segment of all LTP soundings during TC4. The free troposphere is defined from the top of the BL to the ozonopause, as illustrated in Figure 2; (c) same as (b) for  $O_3$  over ACR. The vertical dashed line distinguishes phases of convective activity (greater before 23 July 2007 and after 2 August, diminished in between), as detected in the sondes.

Fig 6 (a) Ozone, RH, temperature profiles at ACR and LTP for 13 July 2007. Vertical bars refer to RW (blue) and GW (green) as described in **Figure 1**. (b) Uv-DIAL image of ozone from DC-8 flight from California to Costa Rica. Ozone < 40 ppbv, purple, is near surface and also at cloud outflow level, ~ 10 km, south of the ITCZ; the latter is the cloudy region at 1945 UTC. Note a thin cloud-outflow ozone lamina at 13 km.

Fig 7 (a) Ozone, RH, temperature profiles at ACR and LTP for 22 July 2007. (b) convective cells with outflow layers denoted by arrows on 22 July 2007 near LTP from ER-2 Cloud Physics Lidar and Cloud Radar System composite image [Hlavka *et al.*, 2010].

Fig 8 Daily mean mixing ratios of (a)  $O_3$ ; (b) CO, from NATIVE in Las Tablas, Panamá (7.8N,80.0N). NATIVE CO readings are higher than the median DC-8 profile data (Figure 2 in Avery *et*

- Fig 9 *al.*, 2010), although NATIVE NO/NO<sub>y</sub> and SO<sub>2</sub> suggest that pollution is infrequent, Profiles from August 2007 TC4 sampling (a) 2 August 2007; (b) 3 August; (c) 5 August. Labels as in Figure 6a. For 5 August, the DC-8 O<sub>3</sub> measurement from profiling near LTP displayed a high-O<sub>3</sub>, low-CO layer [Avery *et al.*, 2010] at 8-10 km. Also on 5 August, the ozonesonde package, caught in dissipating convection, was buffeted in updrafts and downdrafts between 2 and 5 km, presumably due to balloon icing [Morris *et al.*, 2010]. Only the final ascent profile appears in (c), so a GW signal indicating convection does not appear below 7 km. However, the RW segment may denote ozone from pollution.
- Fig 10 (a) Ozone, CO from DC-8 spiral on 3 August 2007 at 1505-1535 UTC, suggests extra-tropical influence at 6-8 km, with convection at 5 km and above 8 km. (b) 3 Aug 2007 ER-2 sampling produced composite CPL-CRS image with convective cells (outflow at horizontal arrows) at 7.5N, 80.5W. Vertical arrows mark LTP sonde launch. (c) Same as (b) except for 5 August.
- Fig 11 Averaged ozone amounts (in DU) in the free troposphere affected by GW, RW determined by the laminar method using all O<sub>3</sub> and P-T-U sounding from J-J-A 1999-2007 for San Cristóbal, Galapagos (0.89S,90W) and Paramaribo, Suriname (5.8N,55E) and, since 2005, for two Costa Rican launch sites near San Jose (Heredia in 2005-2006; Alajuela, ~20 km distant, in 2007). The 2007 data at Las Tablas, Panamá, are from TC4. BL O<sub>3</sub> amounts (not shown) are 2 DU at San Cristóbal, 3.5 DU at Paramaribo and the Costa Rican sites.
- Fig 12 Gravity wave Indices (GWI) based on O<sub>3</sub> and P-T-U soundings from the Paramaribo and San Cristóbal SHADOZ sites.

# Las Tablas, Panama Laminae: 5 August 2007 15Z

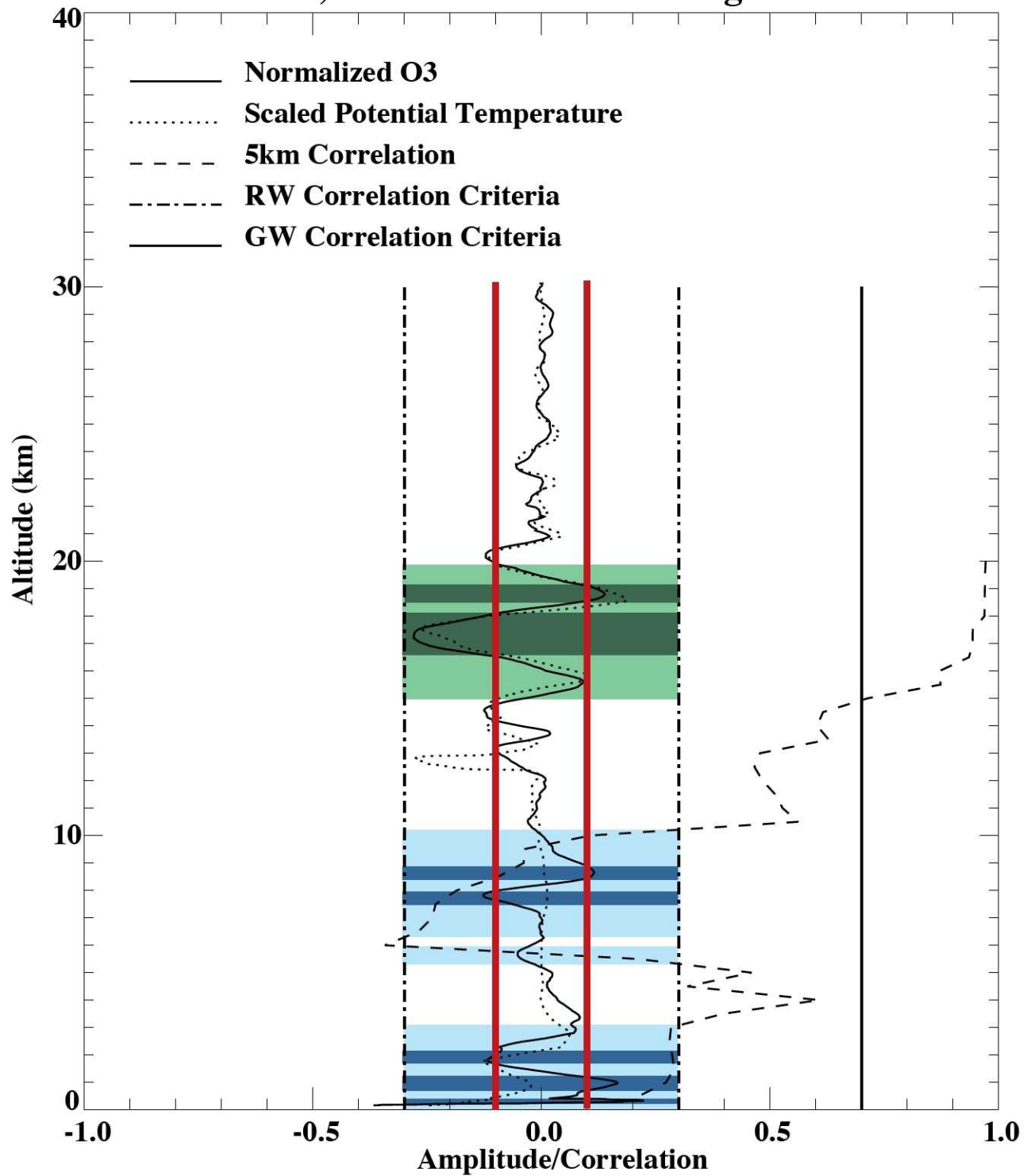
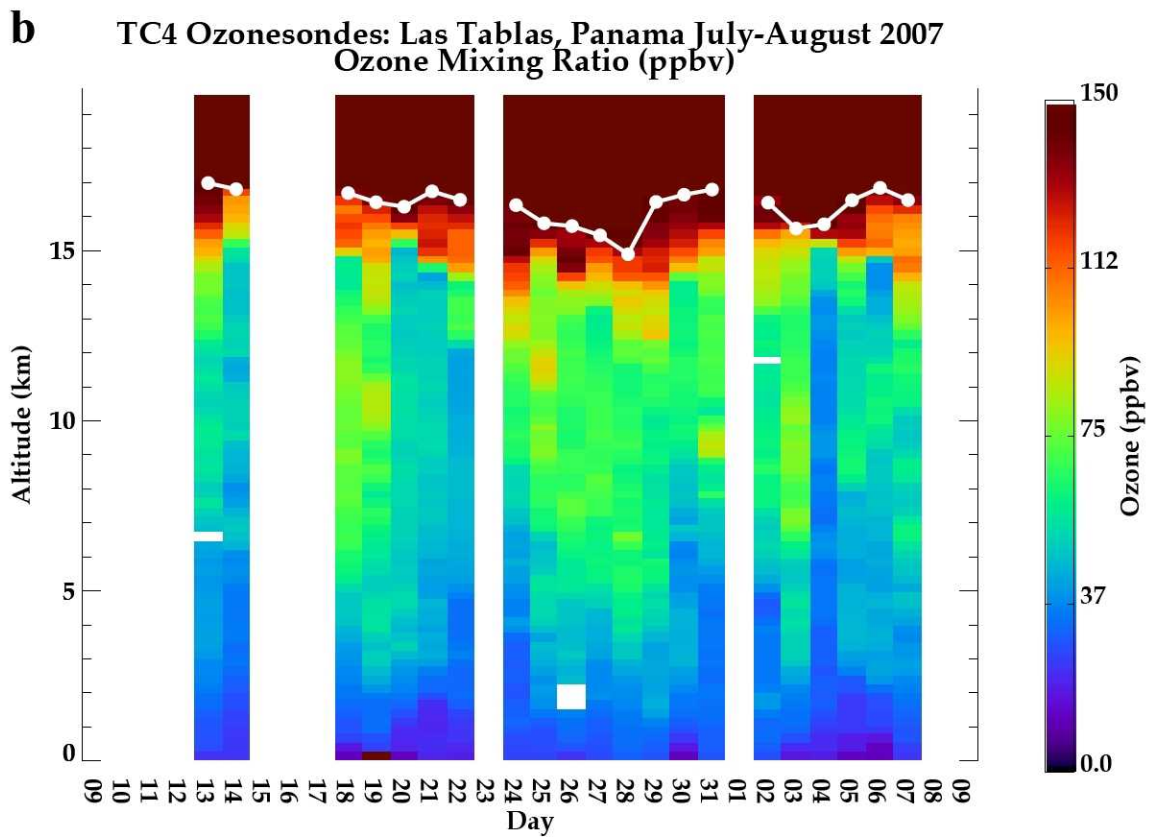
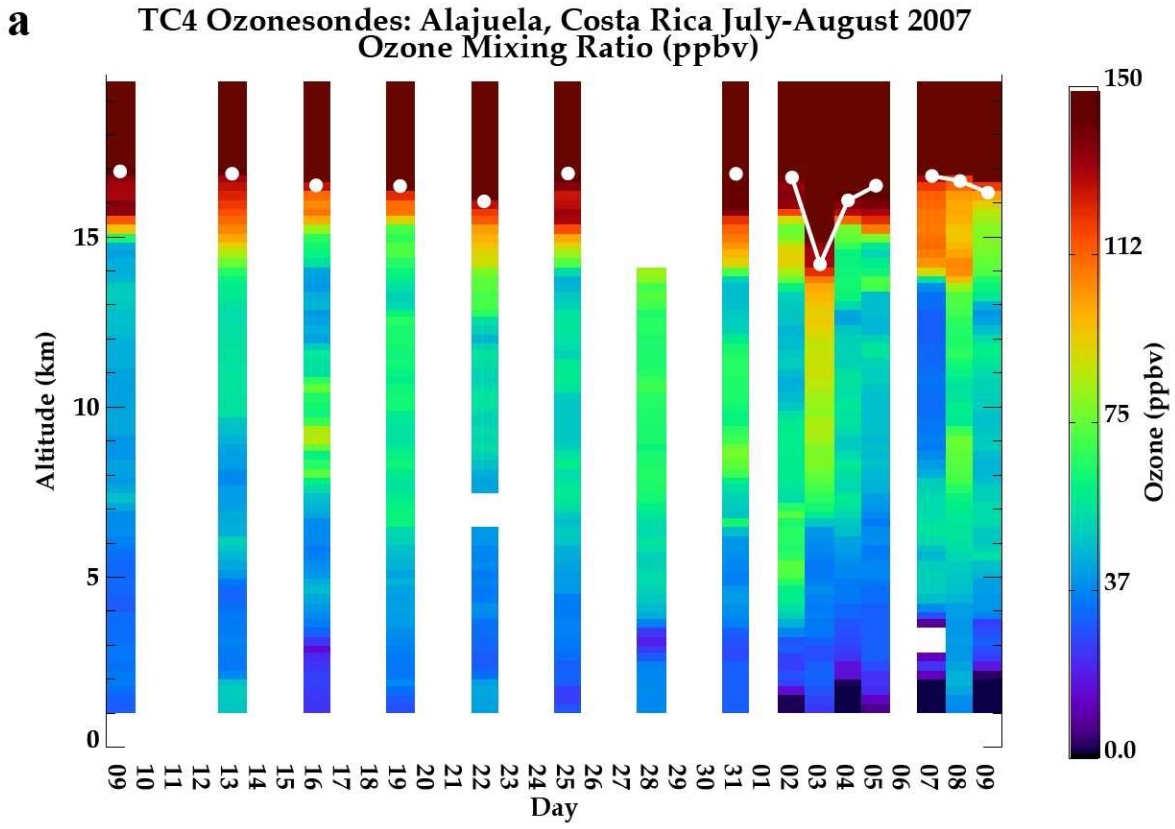
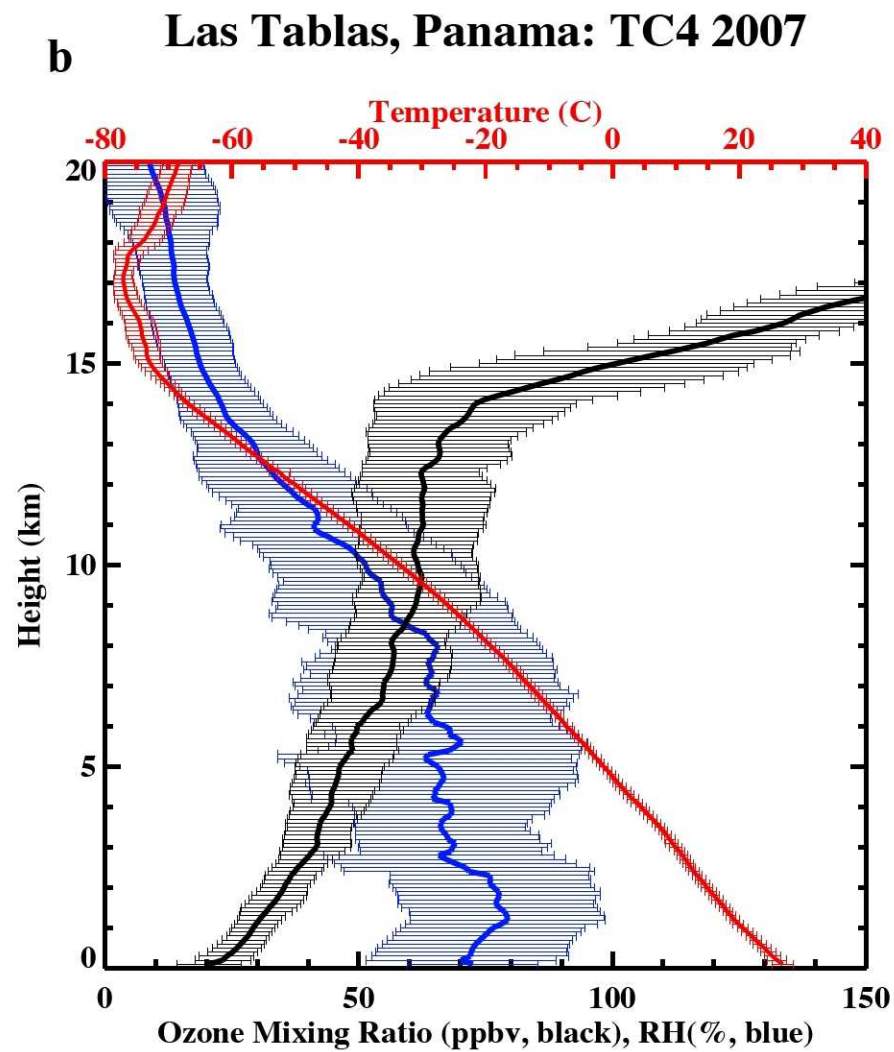
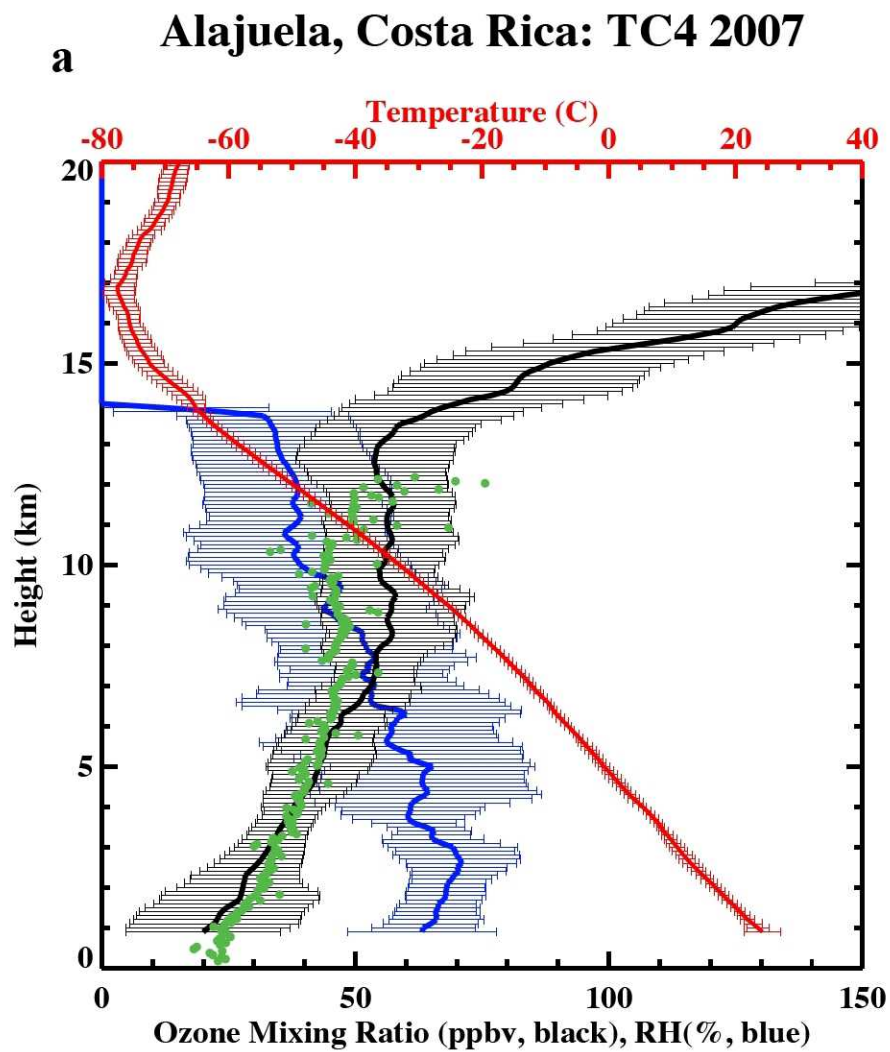


FIGURE 1





**FIGURE 2**



**FIGURE 3**

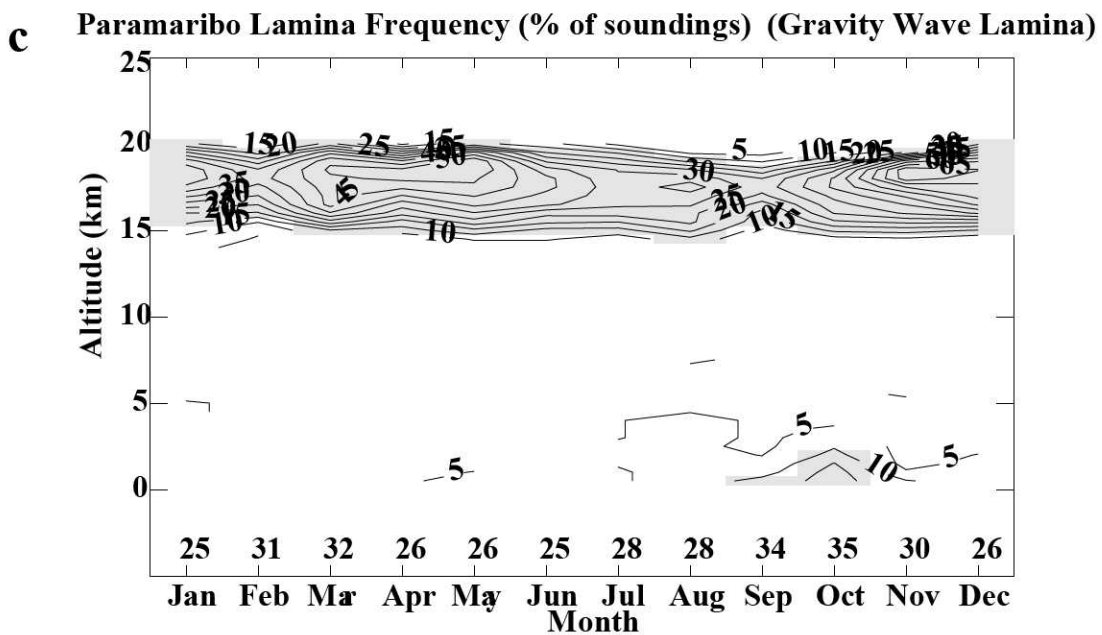
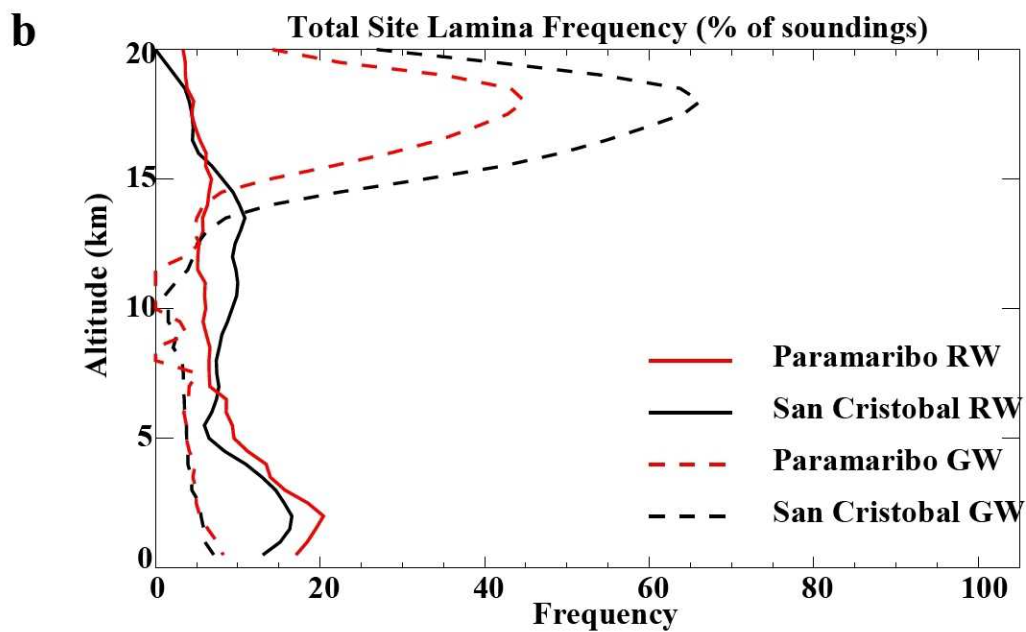
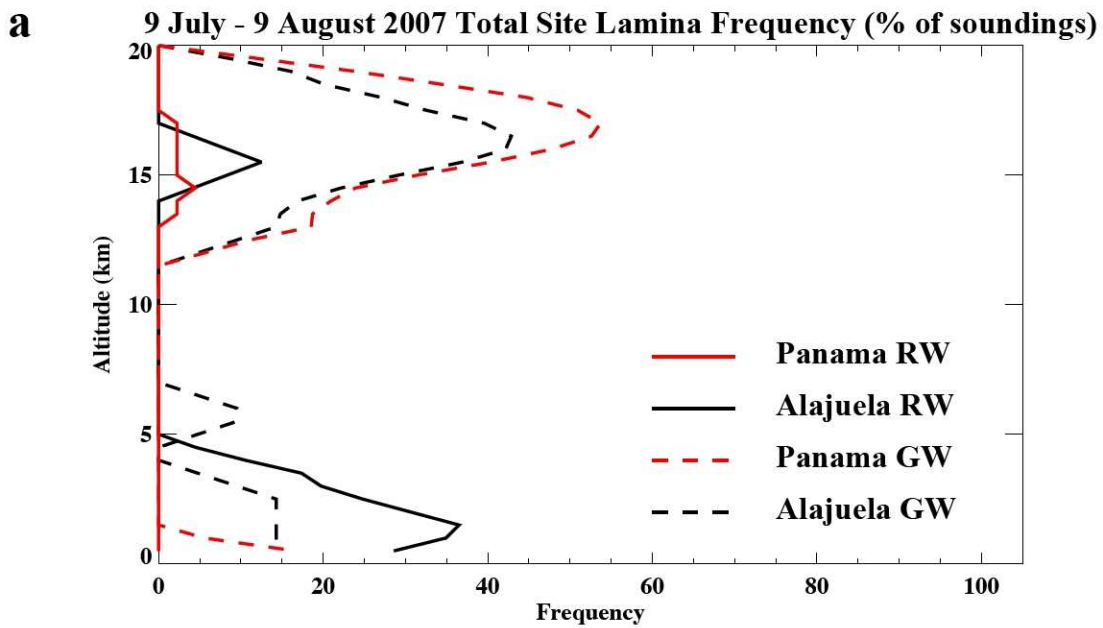
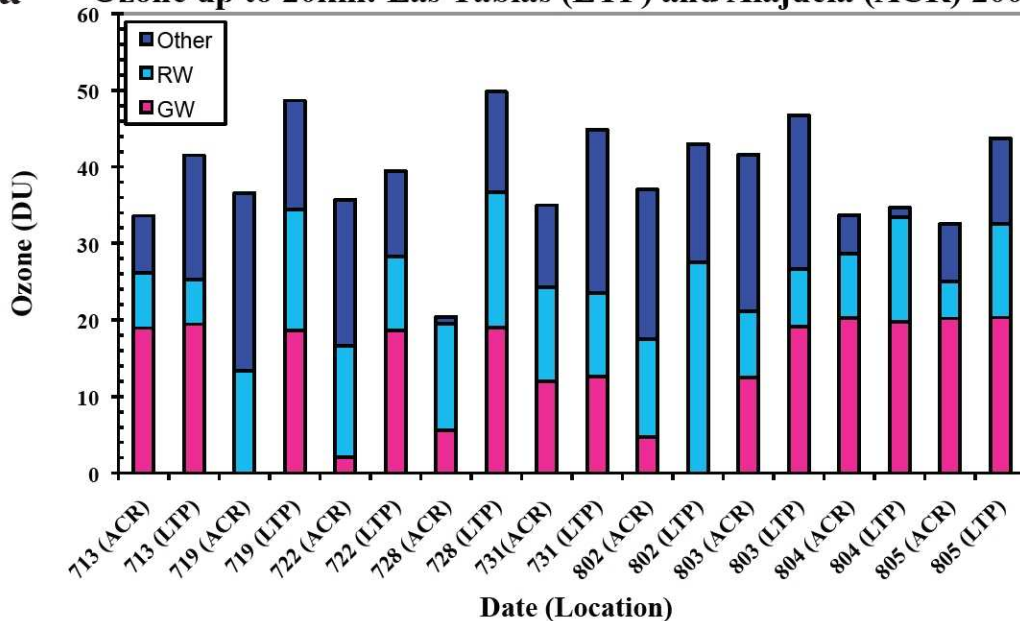
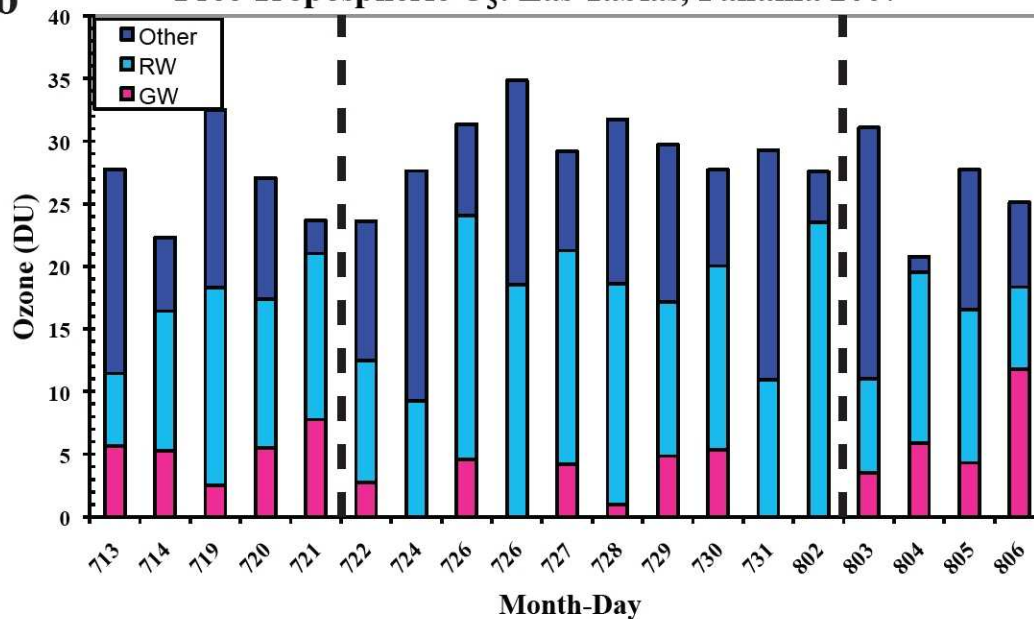


**FIGURE 4**

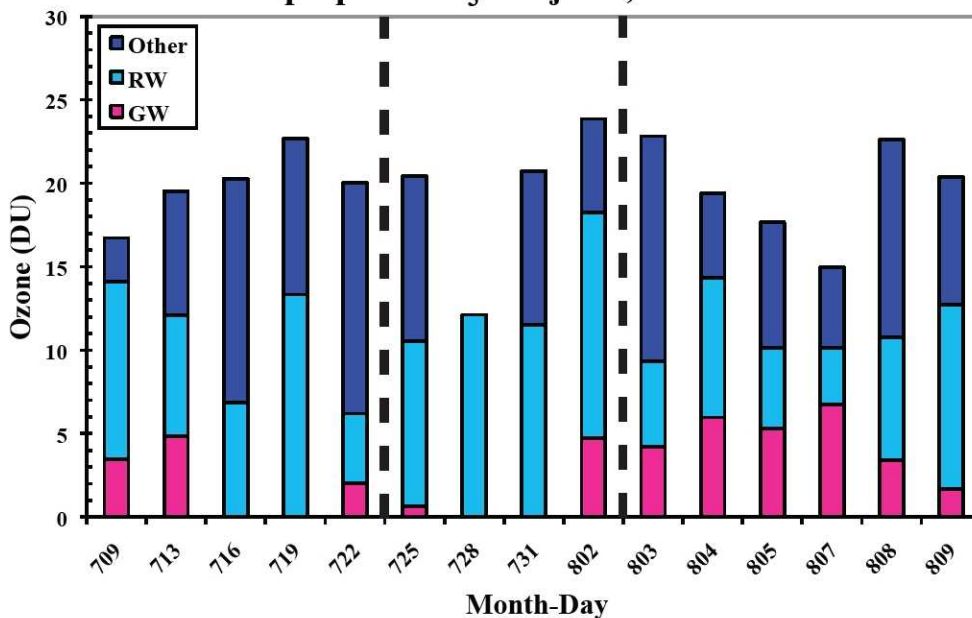
**a** Ozone up to 20km: Las Tablas (LTP) and Alajuela (ACR) 2007



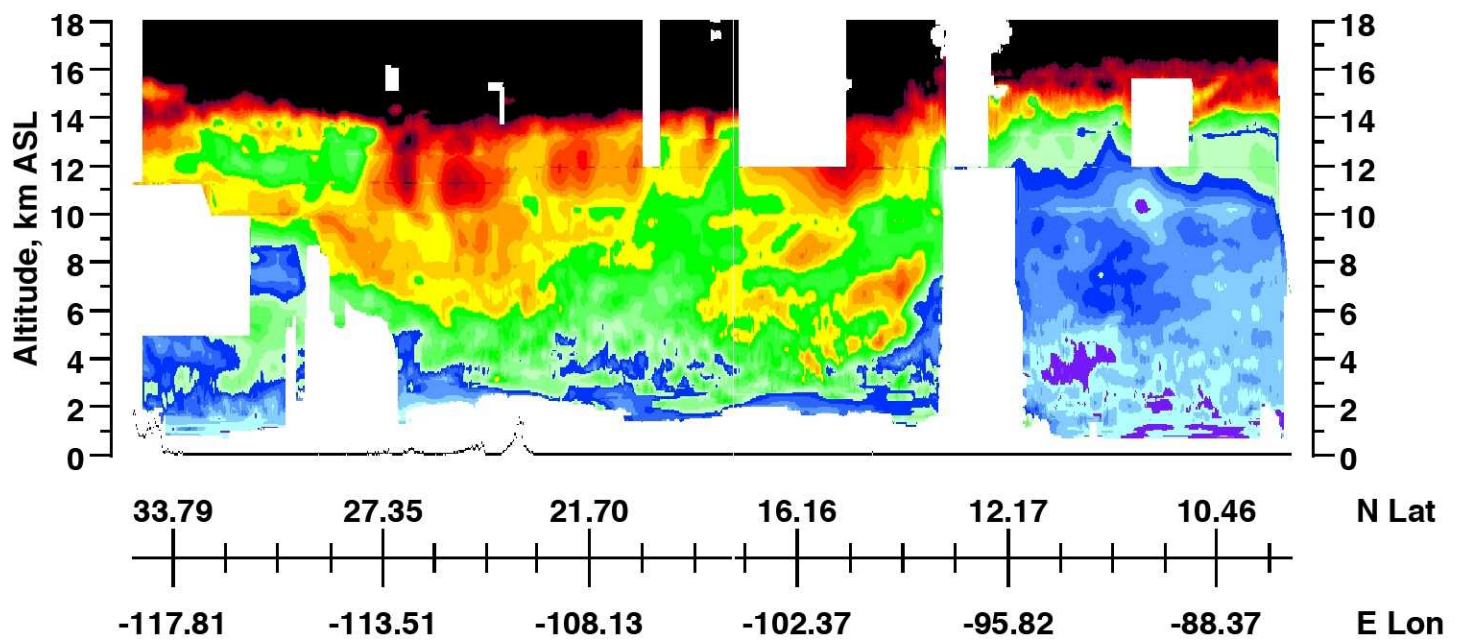
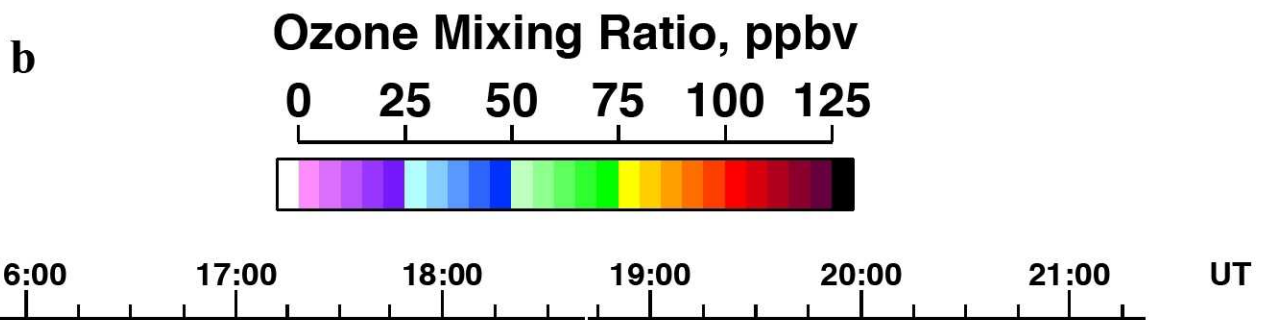
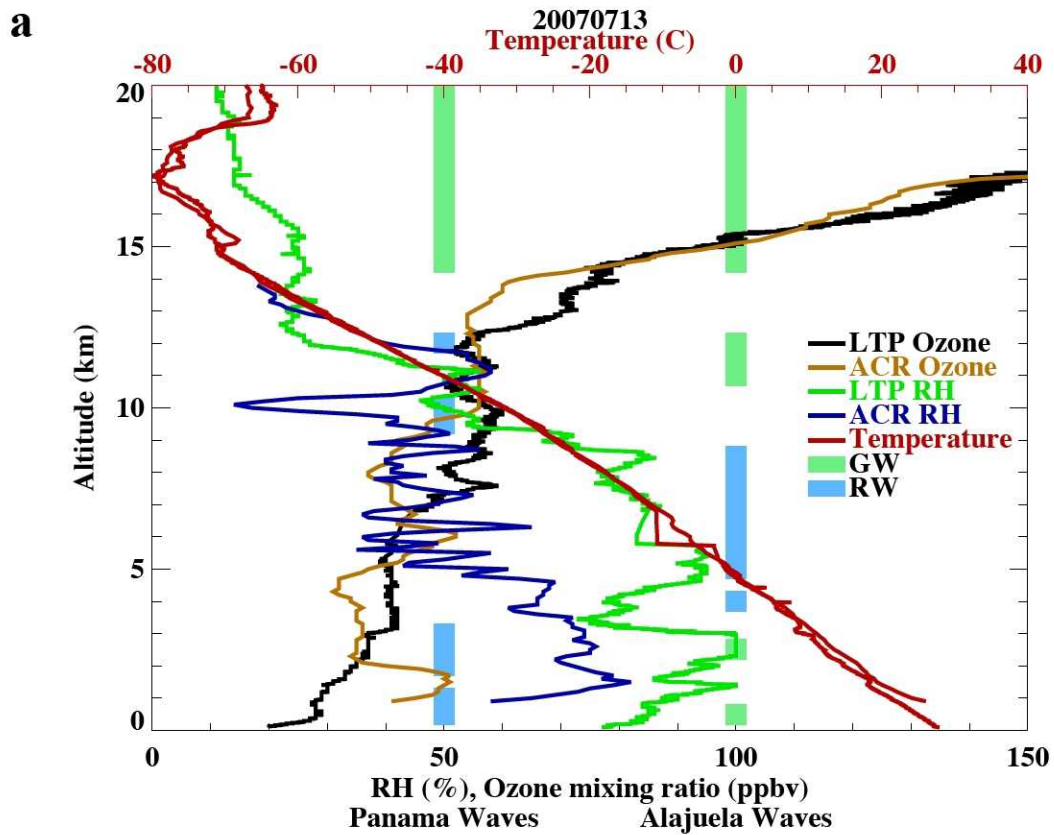
**b** Free Tropospheric O<sub>3</sub>: Las Tablas, Panama 2007



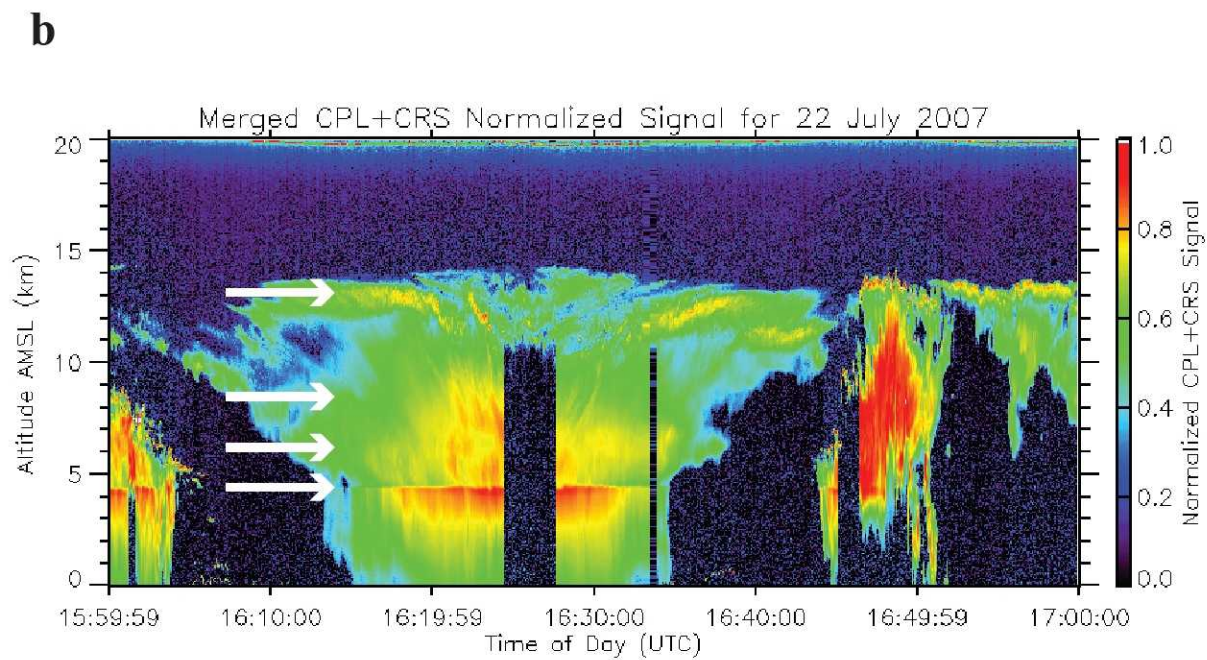
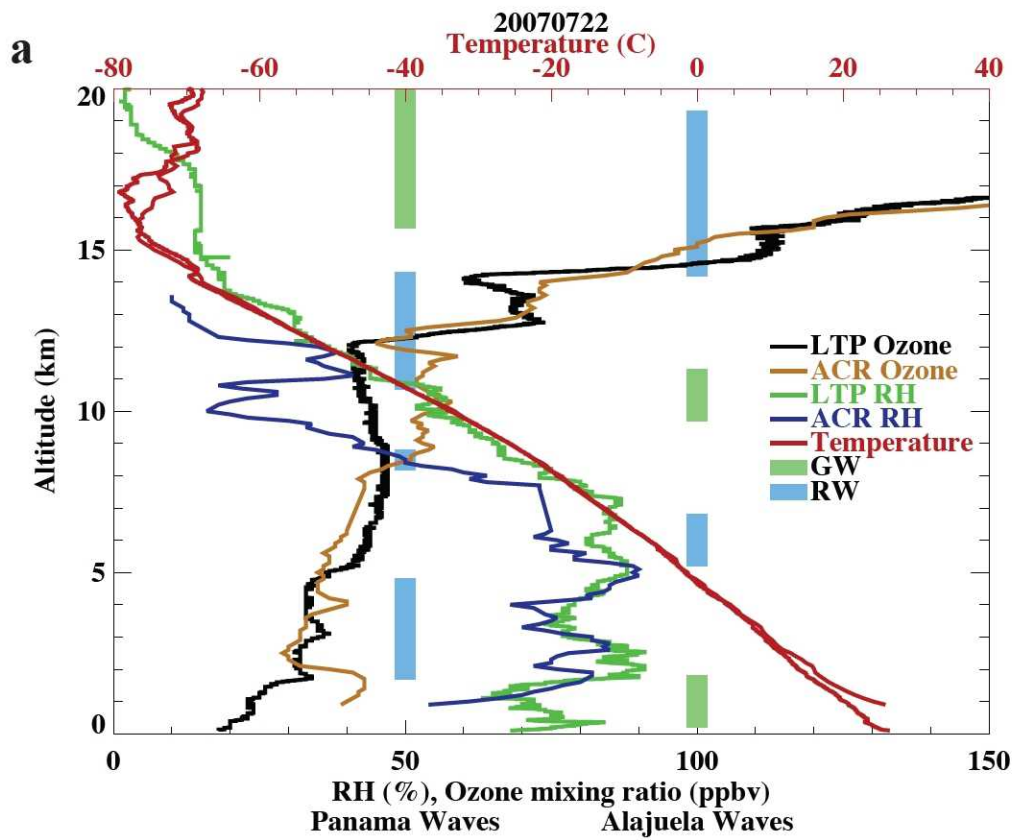
**c** Free Tropospheric O<sub>3</sub>: Alajuela, Costa Rica 2007



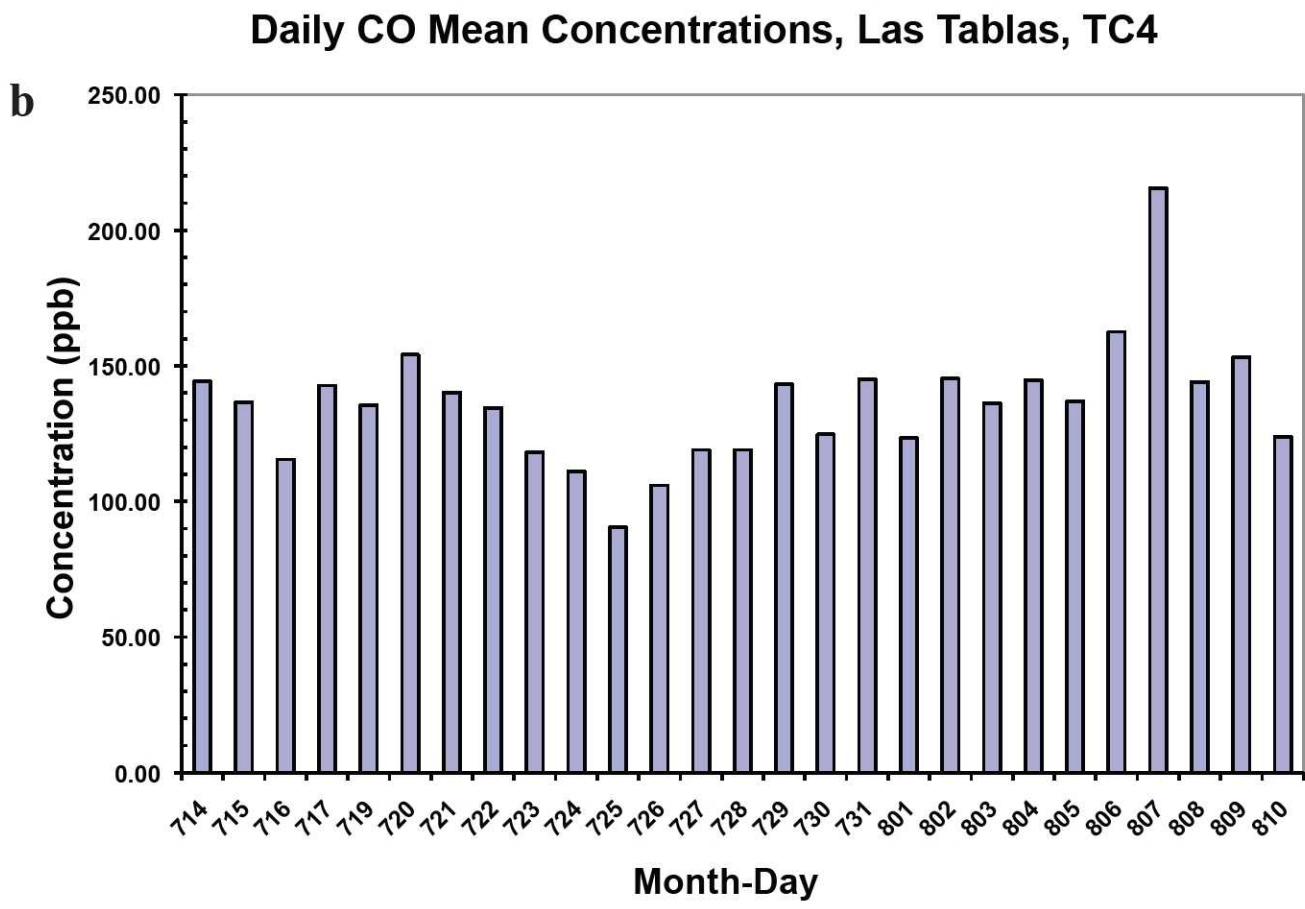
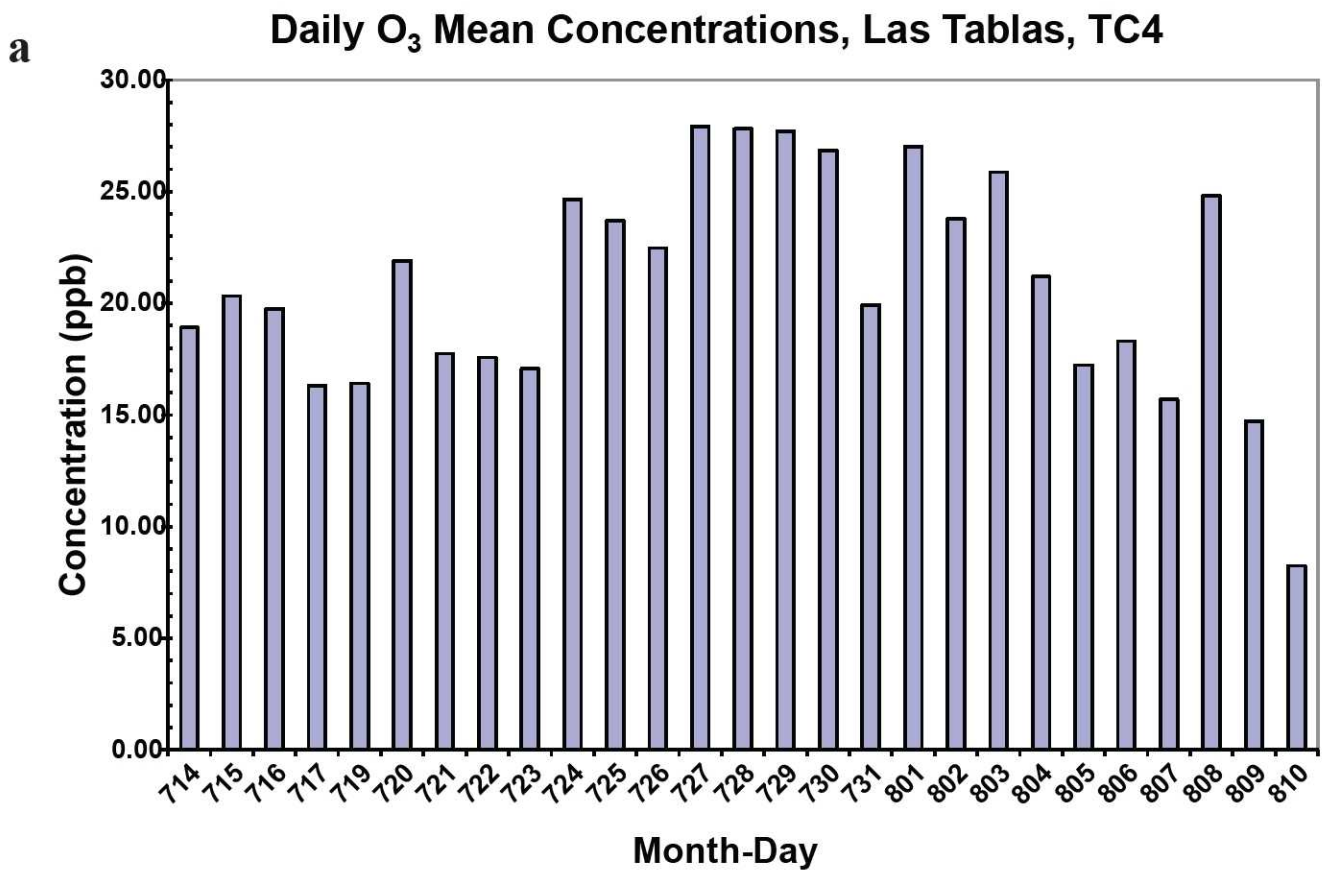
**FIGURE 5**



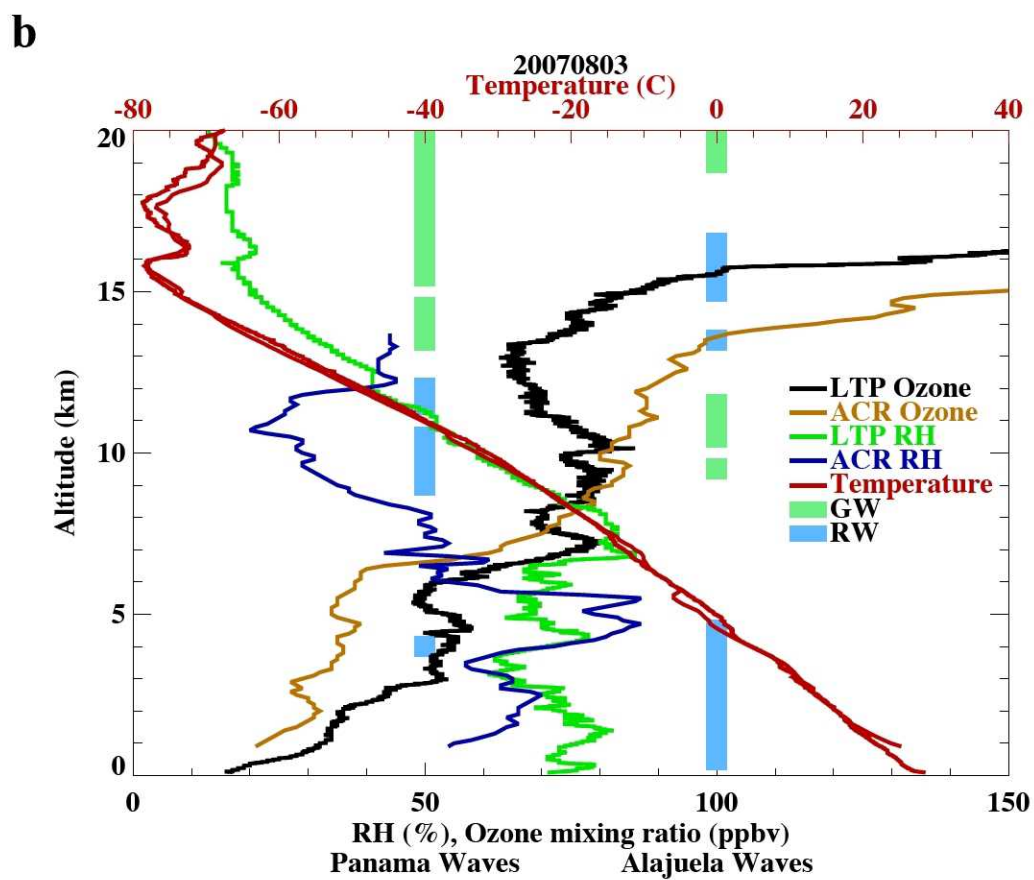
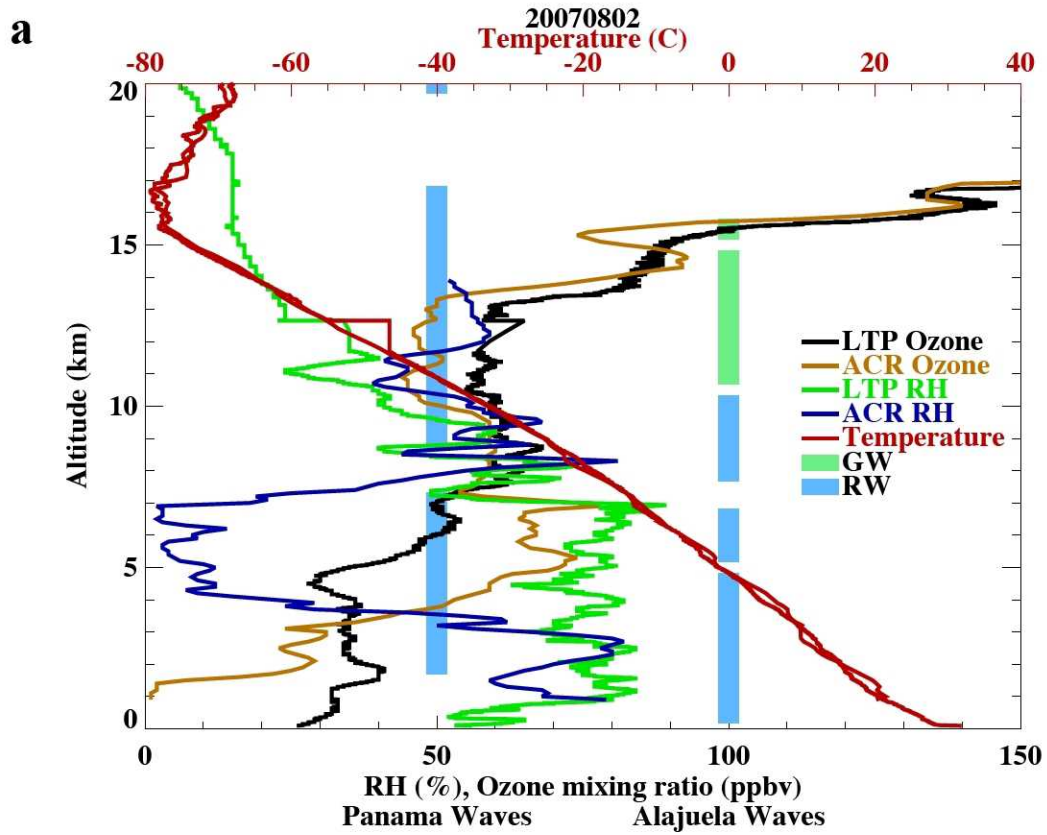
**FIGURE 6**



**FIGURE 7**



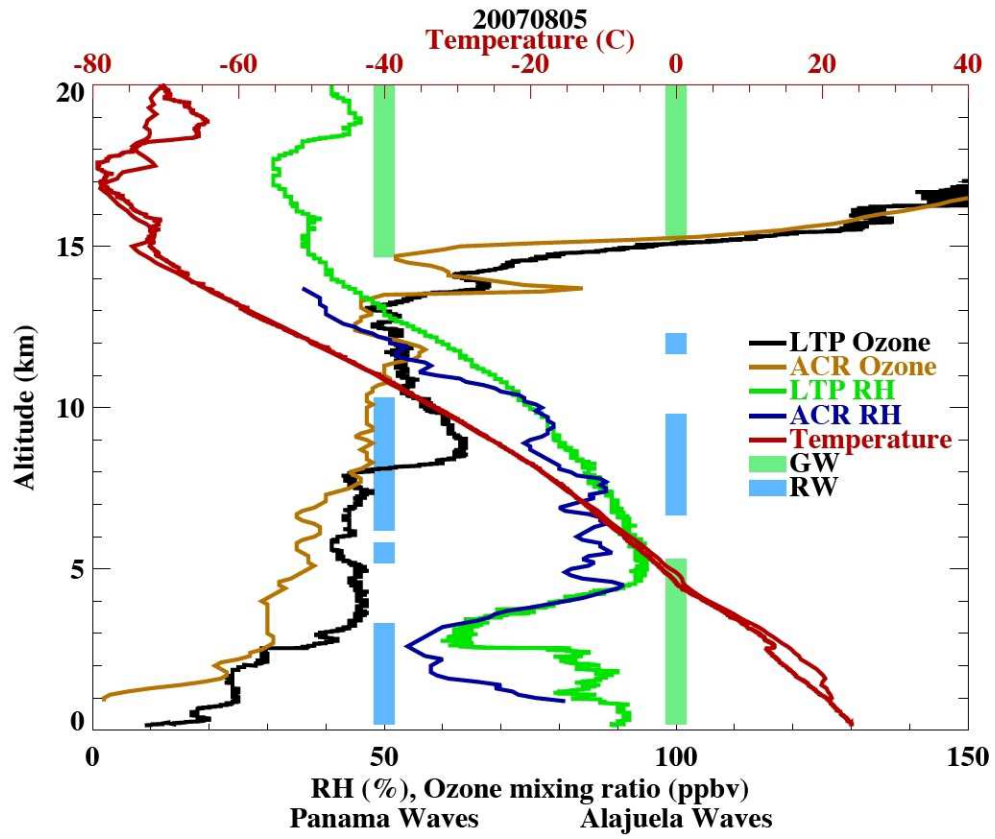
**FIGURE 8**



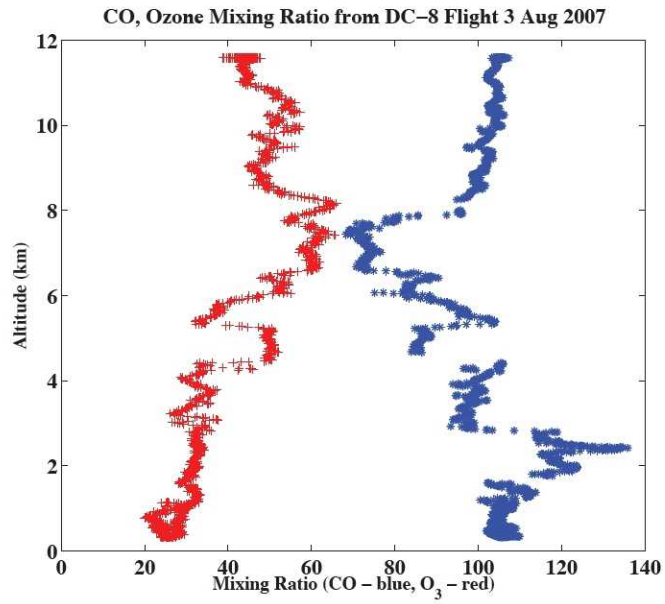
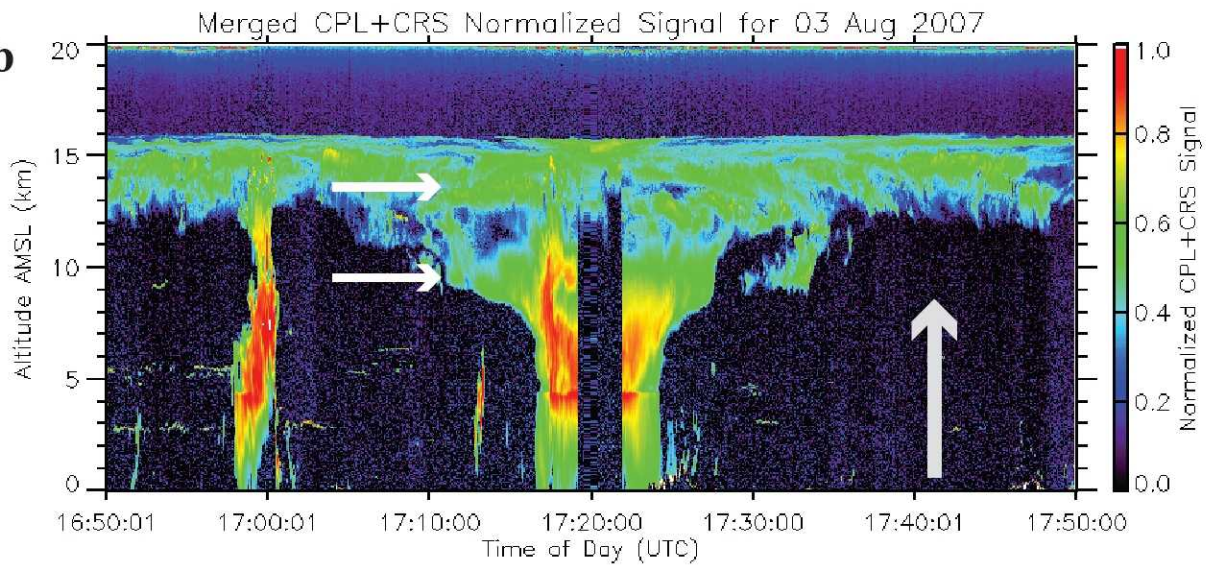
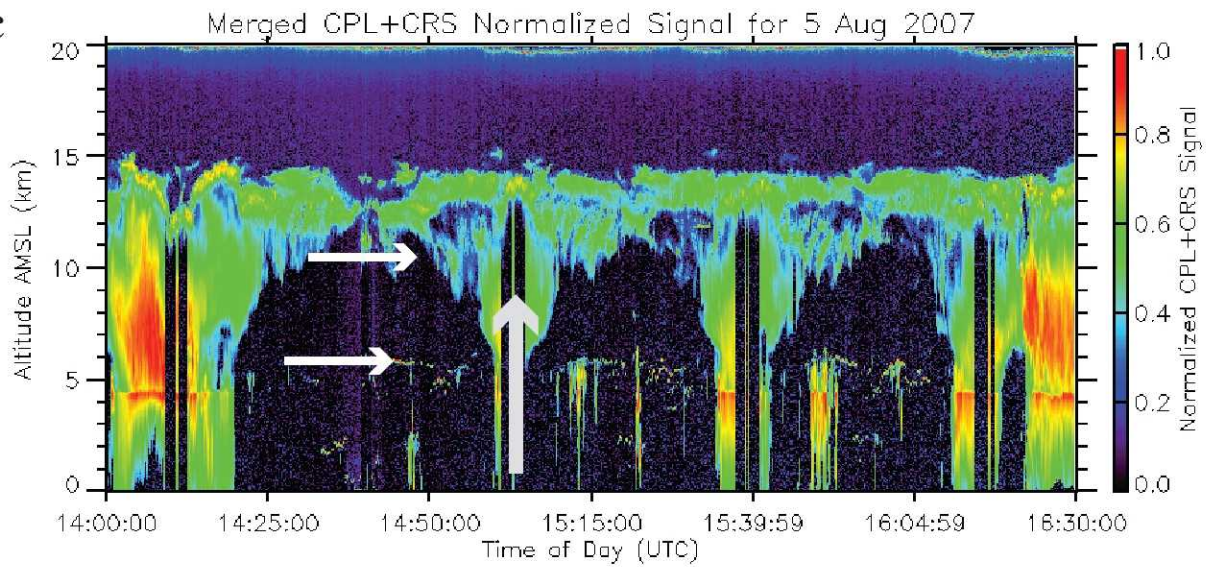
**FIGURE 9**



**C**



**FIGURE 9 (continued)**

**a****b****c****FIGURE 10**

## Mean J-J-A Free Tropospheric Ozone

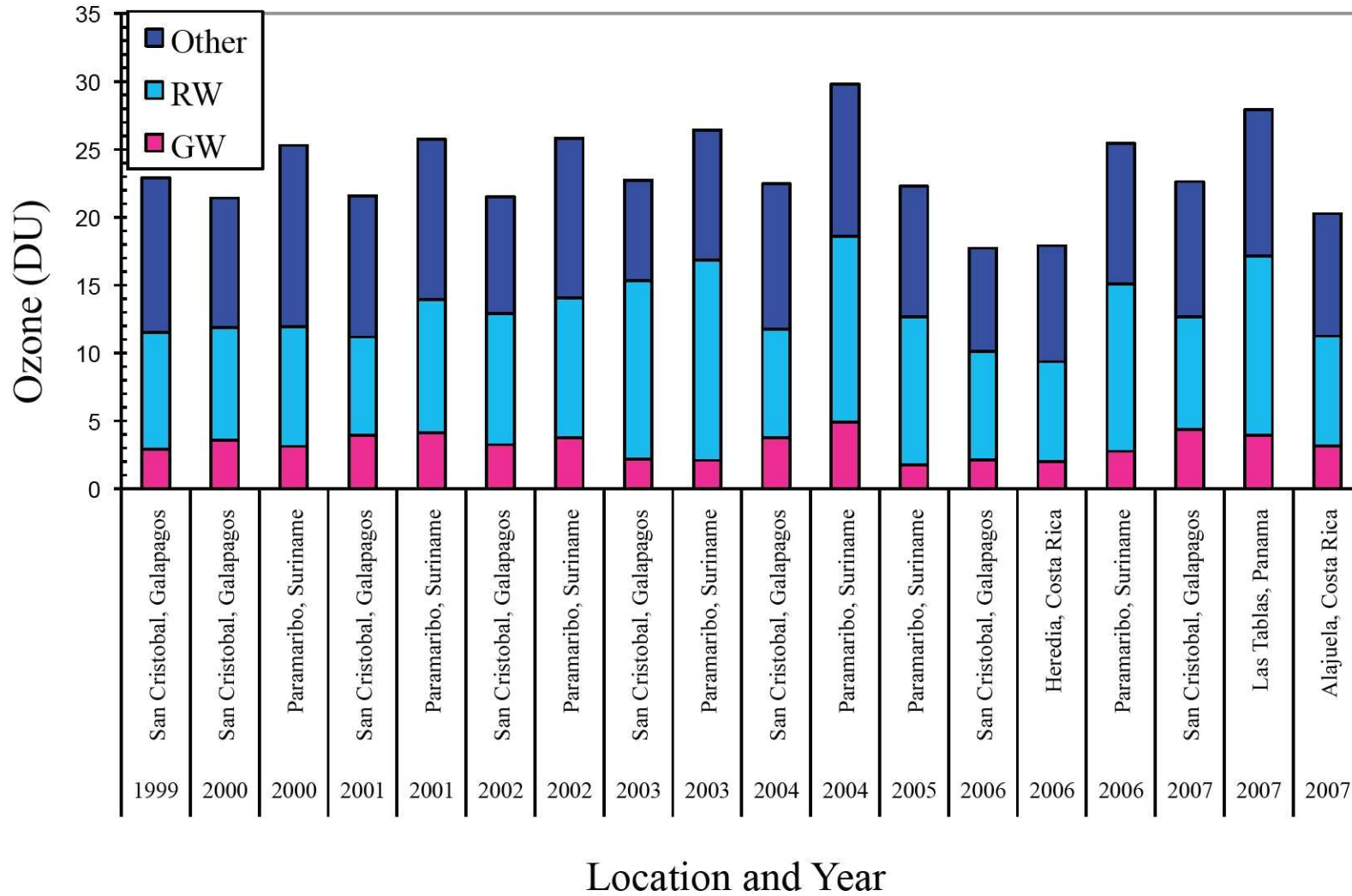


**FIGURE 11**

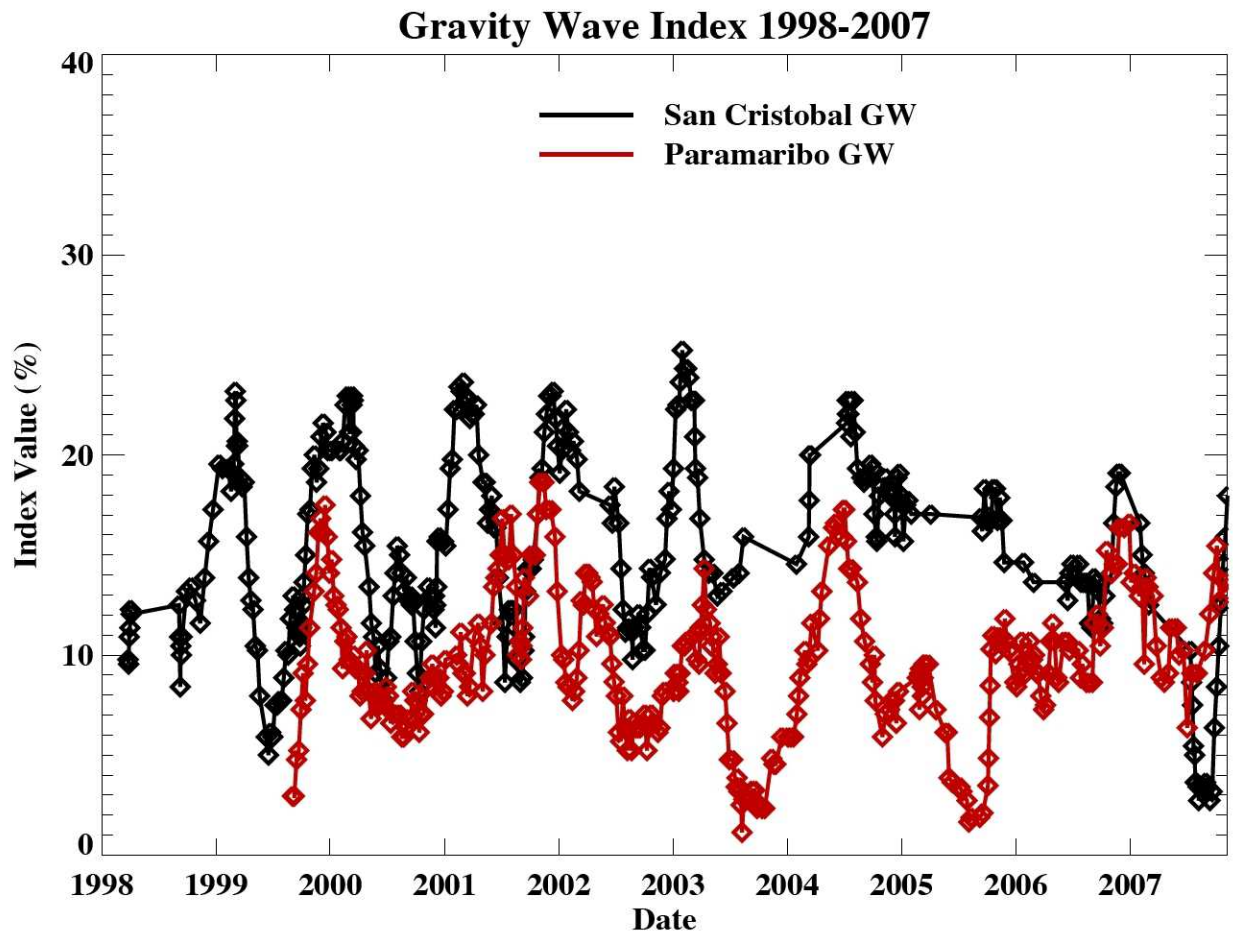


**FIGURE 12**